bioRxiv preprint doi: https://doi.org/10.1101/416677; this version posted September 13, 2018. The copyright holder for this preprint (which was not certified by peer review) is the author/funder, who has granted bioRxiv a license to display the preprint in perpetuity. It is made available under aCC-BY-NC-ND 4.0 International license.

Warm Temperatures, Cool Sponges: The Effect of Increased Temperatures on the Antarctic Sponge *Isodictya* sp.

M. González-Aravena[1]*, N.J. Kenny[2]*^, M. Osorio[1], A. Font[1], A. Riesgo[2], C.A. Cárdenas[1]^

[1] Departamento Científico, Instituto Antártico Chileno, Plaza Muñoz Gamero 1055, Punta Arenas, 6200965, Chile

[2] Life Sciences Department, The Natural History Museum, Cromwell Road, London SW7 5BD, UK

* Authors contributed equally to manuscript
^ Corresponding authors

MGA: mgonzalez@inach.cl
NJK: nathanjameskenny@gmail.com
MO: magdalena.osorio.a@gmail.com
AF: afont@inach.cl
AR: a.riesgo@nhm.ac.uk
CAC: ccardenas@inach.cl

Corresponding author details:
NJK: +44 20 7942 6475
CAC: +56 61 2298124

bioRxiv preprint doi: https://doi.org/10.1101/416677; this version posted September 13, 2018. The copyright holder for this preprint (which was not certified by peer review) is the author/funder, who has granted bioRxiv a license to display the preprint in perpetuity. It is made available under aCC-BY-NC-ND 4.0 International license.

Abstract

Although the cellular and molecular responses to exposure to relatively high temperatures (acute thermal stress or heat shock) have been studied previously, only sparse empirical evidence of how it affects cold-water species is available. As climate change becomes more pronounced in areas such as the Western Antarctic Peninsula, it has become crucial to understand the capacity of these species to respond to thermal stress.

Here we use the Antarctic sponge *Isodictya* sp. to investigate how sessile organisms (particularly Porifera) can adjust to heat shock, by exposing this species to 3 and 5 °C, corresponding to predicted temperatures under the 2080 IPCC-SRES scenarios. Assembling a *de novo* reference transcriptome (90,188 contigs, >93.7% metazoan BUSCO cassette) we have discerned the molecular componentry employed by *Isodictya* to adjust to environmental insult.

Our analyses suggest that TGF-β, ubiquitin and hedgehog cascades are involved, alongside other genes. However, the degree and type of response changed little from 3 to 5 °C, suggesting that even moderate rises in temperature could cause stress at the limits of this organism's capacity. Given the importance of sponges to Antarctic ecosystems, our findings are vital for discerning the consequences of increases in Antarctic ocean temperature on these and other species.

Key Words:

Porifera; Thermal stress; Climate change; Transcriptome; Western Antarctic Peninsula

bioRxiv preprint doi: https://doi.org/10.1101/416677; this version posted September 13, 2018. The copyright holder for this preprint (which was not certified by peer review) is the author/funder, who has granted bioRxiv a license to display the preprint in perpetuity. It is made available under aCC-BY-NC-ND 4.0 International license.

Background

Sponges are vital components of a variety of ecosystems in terms of abundance and ecosystem services[1,2]. This is especially true in the Antarctic, where they are among the most common benthic species, providing habitat and food for a wide range of organisms[3,4,5,6]. Sponges, like most marine species, will be broadly, and perhaps adversely, affected by climate change, but at present studies into their capacity to cope with increases in temperature are limited in scope and number[7,8].

The Western Antarctic Peninsula (WAP) is one of the areas of the planet which has experienced some of the most significant changes in air and water temperature[9,10]. Current estimates of climate change in the Antarctic suggest that the mean temperature of seawater could rise by up to 5 °C by 2080 (IPCC 2014, Table 16.1)[11]. This is expected to have major implications for Antarctic organisms as they have evolved in a very stable and cold environment, being highly sensitive to environmental variation[12,13]. For this reason the projected changes in water temperature constitutes a major threat to ecosystem function in these waters. Such changes would modify the prevalence of key functional species, thus affecting associated ecosystem processes[14]. However, we are only beginning to understand the resilience of many species found in the Antarctic to rising temperature conditions [15,16,17], and the point to which they will be affected by any changes in mean temperature. The deleterious effects of temperature exposure in sponges from other latitudes include bleaching of symbiotes, tissue necrosis and death[18]. It is vital to gain this information in Antarctic sponge species, so that policy decisions can be made with a full understanding of the likely impacts of these changes.

Some sponge species have been suggested to be relatively robust to moderate changes in temperature. Caribbean and Brazilian coral-reef sponges have been investigated and found to survive fluctuations in ambient temperature[19,20]. A recent study, experimentally demonstrated that the boreal deep-sea sponge *Geodia barretti* is able to cope with temperature rises with few ill effects[21]. Other sponge species are however not so resilient [18,22,23], and both reproduction[24] and filtration[25] in sponges has been shown to be affected by increases in temperature. In some cases, this has led to widespread mortality [22,26].

We have little current understanding as to what makes some species able to cope with broad temperature ranges, and it is possible that Antarctic-dwelling species may be particularly vulnerable due to their specialisation for extremely cold, relatively stable temperature conditions[27]. Their molecular cassettes in particular may have altered over evolutionary time, as has been observed previously in a variety of species [17,28,29], and warmer temperatures could

bioRxiv preprint doi: https://doi.org/10.1101/416677; this version posted September 13, 2018. The copyright holder for this preprint (which was not certified by peer review) is the author/funder, who has granted bioRxiv a license to display the preprint in perpetuity. It is made available under aCC-BY-NC-ND 4.0 International license.

prove deleterious. The sponge *Isodictya* sp. (Fig 1A) is no exception to this. While this sponge is commonly observed around the WAP and generally lives in waters with temperatures between -1.8 to 2 °C[30], it is rarely found in warmer areas. Increasingly this sponge is exposed to warmer summer temperatures across its natural range, with shallow-water temperatures reaching 3 °C in some places around the WAP[31]. At present the likely effect of these conditions on sponge species, and in turn the knock-on effects within their ecosystems, are a mystery to science.

A useful means to assay for the ability to cope with rising temperatures in general, and altered molecular responses in particular, is the use of comparative transcriptomic analysis. Illumina-based sequencing can reveal both subtle and broad changes in expression[32]. The decreasing cost of sequencing and steady increase in affordable computational power has made such approaches increasingly viable, even for small lab teams and consortia[33]. These studies have the additional benefit of also providing a suite of information on the genetic componentry possessed by the organism in question, which is particularly useful for non-model species. While genomic-level datasets within the Porifera remain depauperate and limit our understanding of adaptation to particular conditions, a number of investigations into the transcriptomic complements of a variety of sponges have now been successfully performed [34,35,36]. The transcriptional changes in response to temperature shifts that occur within sponges themselves[23,37] and changes in their bacterial symbionts[18,38,39,40.41] have also only recently begun to be unveiled. Some changes in gene expression revealed by these studies, such as those in HSP70 expression[37,42] are easily explained with reference to known metazoan responses to temperature fluctuation. Similarly, responses such as the up-regulation of genes involved in signal transduction, tissue morphogenesis, cell signalling and antioxidant activity are all of clear utility to tissues as they adapt to thermal stresses. What has yet to be tested thoroughly is whether these changes are mirrored in extremophile species, rather than generalists. It is possible that gene complements adapted to extremes may be less able to adapt to changes, particularly at rapid time scales.

Our study demonstrates that extremophile species may be able to respond to moderate temperature increases, but may not have the capacity to adjust further to continued rises in temperature. We have been able to use these findings to investigate the specific pathways used by these organisms, and contrast these with species adapted to warmer temperature regimes. The sponge studied here, *Isodictya* sp. is one of the most common species in shallow-water rocky reefs (<25 m depth) around Doumer Island, Palmer Archipelago, WAP (Fig 1B). This knowledge will be vital for understanding the impact of temperature rises on Antarctic species, but also for discrete, targeted investigation of the role of specific pathways in temperature

bioRxiv preprint doi: https://doi.org/10.1101/416677; this version posted September 13, 2018. The copyright holder for this preprint (which was not certified by peer review) is the author/funder, who has granted bioRxiv a license to display the preprint in perpetuity. It is made available under aCC-BY-NC-ND 4.0 International license.

adaptation in the future. In this manuscript we present the first transcriptomic analysis of the effect of acute warming on a cold-adapted sponge.

Methods

Animal Collection and Heat Treatment

Adult samples of the Antarctic sponge *Isodictya* sp. were collected by SCUBA diving at 10 m depth in Cape Kemp, off Yelcho Research Station, Doumer Island, WAP (64°51′S 63°35′W, Fig. 1B). Sponges were then transferred to the laboratory at Yelcho Station, where they were maintained in 140 L fiberglass tanks with unfiltered, flowing seawater for a week to allow acclimation to laboratory conditions. Tanks were covered with two layers of 1 mm shade cloth (fiberglass 50% neutral density screen) to represent light levels occurring *in situ*. Relative light intensity levels and temperature in the experimental tanks were measured (1 measurement every 15 minutes) during the duration of experiment with a HOBO Pendant® temperature/light data logger (Onset, USA). Sponges were then placed into one of three possible treatment conditions - a control tank, where samples were maintained in seawater pumped directly from the sea floor (5 -10 m depth) at approximately 0.5 °C, or one of two possible treatment temperatures, 3 and 5 °C, with water warmed in a header tank before pumping into the treatment area, and subsequently maintained at a set temperature using SOBO Aquarium heaters (500 watt). Sponge samples were placed in individual treatment tanks, for a total of 6 treatments (2x control, 2x 3 °C, 2x 5 °C) although one control sample was not used for analysis as described in Results and Discussion.

RNA Extraction and Sequencing

Sponges were taken from tanks after 4 hours of exposure to the control/treatment conditions, and a fragment of sample approx. 1 cm^3 was taken immediately and placed in RNAlater (Qiagen) and stored at -80 °C. RNA was extracted from sponge samples using E.Z.N.A Total RNA kit II (Omega Bio-Tek Inc.) according to the manufacturer's protocol with a previous step of homogenization with liquid nitrogen. RNA quality and quantity was determined on a 2100 Bioanalyser (Agilent Technologies). 1 µg from each sample was used to produce RNA libraries for sequencing, with TruSeq Stranded mRNA kit (Illumina), 100bp nominal intra-read fragment size, 15 rounds of amplification and adaptors AGTTCC, ATGTCA, CCGTCC, GTCCGC and CGATGT.

bioRxiv preprint doi: https://doi.org/10.1101/416677; this version posted September 13, 2018. The copyright holder for this preprint (which was not certified by peer review) is the author/funder, who has granted bioRxiv a license to display the preprint in perpetuity. It is made available under aCC-BY-NC-ND 4.0 International license.

Libraries were sequenced on a Hiseq2500 sequencer by the Macrogen provider, using approximately one half of a run in total. The sequencing provider performed initial assessment of read quality and de-multiplexing of reads according to their procedures, and provided us with paired-end reads for download from an external server, with no unpaired orphan reads retained by this process.

Quality Control and Assembly

We confirmed the removal of adapter sequences and overall sequence quality using the FastQC program[43]. Low-quality regions of reads were trimmed using Trimmomatic 0.33[44] with the following settings: ILLUMINACLIP:../Adaptors.fa:2:30:10 LEADING:3 TRAILING:3 SLIDINGWINDOW:4:20 MINLEN:30 where the Adaptors.fa file consisted of the appropriate indexes for the libraries in question. The resulting trimmed reads were then compressed using gzip and re-analysed with FastQC. Seqtk fqchk[45] was used to determine average sequence quality scores.

Trimmed reads from all samples were assembled into a reference transcriptome using Trinity version 2013_08_14[46], with two non-standard settings: a minimum contig length of 200 bp and *in silico* read normalisation. DeconSeq standalone version 0.4.3[47] was used to remove contamination, with settings -i 50 -c 50, using pre-prepared bacterial, archean, hsref and viral databases (2,206, 155, 1 and 3,761 complete genomes respectively), resulting in our final reference assembly. This is available from the DOI and URL below as Supplementary File 1.

Phylogenetic Analysis

28S and HSP70 sequences were extracted from our assemblies using BLASTN[48] on a local server, using sequences of known orthology from Genbank as search queries. These were aligned to previously published sequences downloaded from the NCBI database using MAFFT [49]. HSP70 gene alignments were cured using Gblocks[50], although this was not necessary for the well-conserved 28S sequence. Phylogenetic analysis was run in RAxML GUI[51] using ML + Rapid Bootstrap, the GTR model (28S)/LG+I+G model (HSP70) and 1,000 bootstrap replicates. Phylogenetic and molecular evolutionary analyses of AIF genes were conducted using MEGA version 7.0[52]. The tree was inferred using the Neighbor-Joining method, based on the alignment of the sequences using ClustalW 2.0[53] (alignment was improved using the Seaview software 4.6.5[54]). Resultant tree topologies were evaluated by bootstrap analyses based on 1000 replicates.

bioRxiv preprint doi: https://doi.org/10.1101/416677; this version posted September 13, 2018. The copyright holder for this preprint (which was not certified by peer review) is the author/funder, who has granted bioRxiv a license to display the preprint in perpetuity. It is made available under aCC-BY-NC-ND 4.0 International license.

Transcriptome analysis and annotation

To assess the content of the transcriptome BUSCO v1.1b1[55] was run against the reference transcriptome, using the eukaryotic and metazoan Basic Universal Single Copy Orthologue (BUSCO) cassettes to estimate completeness. Annotation of contigs was performed by translating the longest ORF for each contig using the getORF.py python script, taking the longest ORF, then using standalone BLASTP[48] (cutoff *E* value 0.000001) to search against the refseq protein database. This was supplemented using Blast2GO Pro[56], where full InterPro scanning, mapping, annotation (including ANNEX) and enzyme code mapping was performed, the complete annotations for which are available as Supplementary File 2.

The KAAS-KEGG automatic annotation server was used to gain an understanding of the recovery of complete pathways in our transcriptome. These were generated using the online tool[57] rather than as integrated into Blast2GO, due to the increased functionality of the standalone server. The bi-directional best hit method was used to identify and annotate the longest orfs from our contigs, with the protein sequences generated earlier used as the basis for these comparisons against a range of eukaryotic species. The maps generated by this were compared directly against extant ones previously generated for the sponge *Amphimedon queenslandica,* and the complete annotations are available as Supplementary File 3.

Differential Expression Analysis and Over-representation Analysis

Comparative analyses of gene expression were performed using RSEM[58] as packaged within the Trinity module, using Bowtie2[59] for alignment. The three treatments (control, 3 and 5 °C) had their replicates cross-sample normalised according to Trimmed Mean of M-values. The three treatments were then cross-compared using edgeR[60] with a p-value cut off for FDR of 0.0001, a min abs(log2(a/b)) change of 2 (i.e. 4 fold change) and a dispersion setting of 0.1. We excluded any differentially expressed contigs where transcription was only detected in a single sample of any of the five used in this analysis, prior to clustering, to avoid spurious results caused by transient expression or contamination of single samples. The remaining differentially-expressed gene lists were then targeted for further analysis. These results are provided as Supplementary File 4.

GO over-representation analysis was performed in Blast2GO Pro[56] using Fisher's Exact Test, with FDR control for multiple testing, with a p-value cutoff of 0.05[61]. The test sets were the annotated results for the sequences present in each of the over-represented sets derived from the differential expression analysis, analysed in turn, with the reference set the full list of annotated contigs, minus those in the test set.

bioRxiv preprint doi: https://doi.org/10.1101/416677; this version posted September 13, 2018. The copyright holder for this preprint (which was not certified by peer review) is the author/funder, who has granted bioRxiv a license to display the preprint in perpetuity. It is made available under aCC-BY-NC-ND 4.0 International license.

Results and Discussion

Sequencing and Read Cleaning

While 5 individual samples are noted here (a single control, and two replicates for both the 3 °C and 5 °C treatments) another control sample was also initially taken and sequencing performed as described above. Despite being morphologically identical, our initial assays of the sequences from that sample, and particularly the sequence of common molecular markers used in phylogenetic comparison, including *28S rRNA* and *cytochrome c oxidase 1* (*CO1*) markers, revealed that it is in fact a cryptic related species, which will be the subject of description in the future (see Fig. 1C). We have therefore not included this sample in any of the further analyses described in this work.

Basic sequencing metrics can be seen in Table 1, alongside those after read cleaning. Our initial FastQC analysis revealed the presence of low quality nucleotide sequence in the second file of many pairs. Cleaning was therefore stringent, and resulted in markedly fewer, but much better average quality, reads for all samples, which were then used for assembly of the reference transcriptome and for differential expression analysis. GC% (which can be a crude proxy for contamination or changes in expression) was even through all our samples, between 44 and 46%, and changed little with cleaning. A small number of over-represented sequences were also initially observed in our reads, as is commonly observed in Illumina-based transcriptomic analysis due to known biases in hexamer binding[62]. The difference in average quality after cleaning was modest, with an average difference of around 2 in Phred score, but this difference will be due to the removal of error-prone reads (see total number of reads retained) and we are confident that mapping results benefitted from the stringent cleaning process, which prevented both mis-assembly in the *de novo* assembly and mis-alignment in the course of read mapping. Our original reads have been uploaded to the NCBI SRA with accession number PRJNA415418.

Assembly and Completeness

Reads from all 5 samples were used to construct a reference assembly, for use in further analysis (Supplementary File 1). We checked this for potential contamination using Deconseq, comparing our data to known bacterial, viral, 'archaea' (*sensu* [63], we are aware of archaean paraphyly) and human genomic sequences. With very permissive settings for recognition as foreign sequence (minimum thresholds for removal, 50% similarity across at least

bioRxiv preprint doi: https://doi.org/10.1101/416677; this version posted September 13, 2018. The copyright holder for this preprint (which was not certified by peer review) is the author/funder, who has granted bioRxiv a license to display the preprint in perpetuity. It is made available under aCC-BY-NC-ND 4.0 International license.

50% of the contig length) 797 contigs were tagged as potential contamination. These were removed from our dataset before further analysis. It should be noted, however, that particularly novel bacterial sequences not yet represented in the *nr* database may still be present in our data, despite the use of polyA sequencing, as these could not be represented in our removal database and therefore will not have been removed. While beyond the scope of this manuscript, changes in symbiont content may be vital for long-term adaptation to change, and these may be of interest to future study.

Statistics related to our cleaned reference assembly can be seen in Table 2, and the distribution of size and GC% can be seen in Fig 2. A total of 90,188 contigs are present, and Trinity, a splice aware assembler, has automatically assigned 70,844 as independent "genes". A small amount of heterozygosity or potential splice variation has therefore been recognised by the assembly software, with 19,344 contigs flagged as isoformal variants of other contigs in our assembly. This is not unusual, and is in fact less than that recognised in some other *de novo* assemblies (for instance, where every gene possessed approximately 2 "isoform" variants on average[64]). Our samples may therefore possess little in the way of genetic variability at most loci. Our reference assembly is well-assembled, with a high N50 (1,113 bp) sufficient to span the full length of many protein coding genes. 12,997 contigs were longer than this N50 value, and 14,633 longer than 1kb in length. Given that the expected complement of genes in most metazoans is around 20,000 in quantity, a significant number of these are likely to be represented in these well-assembled contigs.

To test the completeness of our transcriptomic dataset we used the BUSCO approach[55]. BUSCO analysis revealed our dataset to be remarkably complete (Fig 2, top right). Of 978 BUSCO groups plausibly expected in any metazoan species, 916 complete BUSCOs were found (654 single copy, 262 duplicated, possibly reflecting allelic or isoform differences). 20 were present only as fragmentary sequence, while 42 were missing. Of the 303 eukaryotic BUSCO sequences, 298 (98.4%) were present, 213 as single copy, 85 with duplicates and 2 as fragmentary sequence. Only 3 BUSCO groups were missing. By way of comparison, the published draft of the *Amphimedon queenslandica* set is missing 1.6% of the eukaryote set (5 genes), and 4.9% (49) of the metazoan complement[36]. Our transcriptome therefore compares favourably with that resource.

Annotation and Content

To annotate our data, we used a number of automated methods, built around the Blast2GO Pro and KEGG platforms. Of 90,188 total contigs, 20,607 were given an initial

bioRxiv preprint doi: https://doi.org/10.1101/416677; this version posted September 13, 2018. The copyright holder for this preprint (which was not certified by peer review) is the author/funder, who has granted bioRxiv a license to display the preprint in perpetuity. It is made available under aCC-BY-NC-ND 4.0 International license.

annotation based on BLAST results *vs*. the Refseq database. Of these contigs, 7,303 had their "best hit" to proteins in the *A. queenslandica* genome. No other species had more than 1,000 contigs with "best hits" to their complements, but the cnidarian *Nematostella vectensis,* a variety of invertebrate deuterostomes (*Branchiostoma floridae, Saccoglossus kowalevskii* and *Strongylocentrotus purpuratus)* and lophotrochozoan species (*Crassostrea gigas, Aplysia californica* and *Lottia gigantea)* were the next most commonly represented metazoan species in this group. This likely represents the relatively slow rate of molecular evolution in these clades when compared to model species such as *Drosophila melanogaster* and *Caenhorhabditis elegans*. The diatoms *Phaeodactylum tricornutum CCAP 1055/1* and *Thalassiosira pseudonana CCMP1335* were observed as "best hit" species for 798 and 563 contigs respectively, which is not surprising as previous work as described abundant presence of diatoms in other Antarctic sponges [65,66]. Annotated diatom data was not included in further analysis. No obvious bacterial, viral, human or archaeal contamination was observed.

More discrete annotation was then performed using Blast2GO Pro. Of the 20,607 contigs preliminarily annotated with Blast, 6,267 could not be annotated further. 12,924 contigs received GO annotations, and were thus fully annotated by this process (Supplementary File 2). 1,389 were able to be "mapped" to GO terms. 27 had Interproscan results and were placed into GO categories. While the expected total gene complement of a metazoan is often up to around twice this figure, our annotations are nonetheless a sizable proportion of the expected total gene count of these sponges. It should be noted that only genes with known and annotated homologues in other organisms will be represented in this contingent - as Blast2GO relies on Blast similarity and extant databases, any novel genes will not be well annotated by this process, and we anticipate that a number of the contigs without blast results will be identifiable in the future, as databases and automated methods of gene identification continue to improve.

We also performed KEGG annotation on our *de novo* transcriptome, to understand the representation of key pathways in our transcriptomic datasets. The results of these annotations are provided in full as Supplementary File 3, but in general recovery was excellent with 37,313 genes annotated to existing KEGG terms. While sponges do not possess the full canonical complements of other metazoan phyla, as these were not present in the common ancestors of sponges and the broader Metazoa, we generally recover the expected gene complements of the Porifera in our reference transcriptomic assembly, when mapped to the *A, queenslandica* KEGG dataset. Together with BUSCO results and the raw number of annotated genes, this gives us confidence in the depth of our transcriptomic resources. We have used these KEGG maps for detailed examination of key signalling and regulatory pathways, as discussed further below.

bioRxiv preprint doi: https://doi.org/10.1101/416677; this version posted September 13, 2018. The copyright holder for this preprint (which was not certified by peer review) is the author/funder, who has granted bioRxiv a license to display the preprint in perpetuity. It is made available under aCC-BY-NC-ND 4.0 International license.

Differential Expression Results

We utilised our samples to perform a differential expression analysis, aimed at discerning the specific genes up- and down- regulated by exposure to acute increased temperatures. The sample correlation matrix and heatmap of relative expression for differentially expressed genes can be seen in Fig 3. While replicate samples at 3 °C correlated almost identically with one another, there was slight fluctuation between our 5°C replicates, perhaps due to inter-individual differential responses to these challenging conditions. The large degree to which the 3 and 5 °C treatments resemble one another can be seen in the matrix in Fig. 3A, where the 4 replicates show little differentiation from one another (black regions of matrix). In Fig 3B, while some discreet inter-sample variation is observed, note the large downregulated quadrant of the matrix at bottom right, relative to high relative expression levels in the control sample at far left.

In general, we found a large number of genes whose expression was perturbed by heat treatment at both 3 and 5 °C. Between our control and 3 °C treatments, the transcriptional landscape changed significantly, with 1,435 contigs changing significantly in expression (767 upregulated, 668 downregulated at the 3 °C treatment compared to the control sample). This was mirrored in our control *vs.* 5 °C comparison, where 1,230 contigs changed significantly in expression (623 upregulated, 607 downregulated significantly at 5 °C compared to control sample). The complete list of differentially expressed genes and further details are given in Supplementary File 4. There was a significant amount of overlap between these sets. In total, 322 genes were downregulated commonly in both the 3 and 5 °C samples when compared to the control. 383 genes were upregulated commonly in both the 3 and 5 °C samples compared to the control. It is these genes that may be particularly interesting for further analysis, given their conserved role in thermal response, and we have provided these in Supplementary File 5.

The 20 most up and down regulated genes in our control vs 3 °C and control vs 5 °C samples are of clear interest in understanding thermal stress response, and can be seen in Table 3. These contigs include those with similarity to heat shock proteins (*heat shock 70 B2-like*) and ribosomal proteins (*40S ribosomal S13*, *40S ribosomal S25*), along with a large number of sequences with no clear homologues in the RefSeq database, and some of less clear utility (e.g. the *Plant Cadmium Resistance 3-like* family of eukaryote-conserved genes, although cadmium and these genes are noted to influence the HSP pathway[67]).

However, very few genes (5 upregulated in 5 °C sample vs 3 °C, 11 downregulated) changed significantly in expression between the 3 and 5 °C treatment. We speculate that this

bioRxiv preprint doi: https://doi.org/10.1101/416677; this version posted September 13, 2018. The copyright holder for this preprint (which was not certified by peer review) is the author/funder, who has granted bioRxiv a license to display the preprint in perpetuity. It is made available under aCC-BY-NC-ND 4.0 International license.

may be due to the transcriptional machinery of this sponge already operating at maximum capacity to adjust to thermal stress under the 3 °C treatment, with little extra ability to cope with changes brought by further increases in temperature. Despite their small number, these genes are of a variety of annotations, including *allograft inflammatory factor 1*, *ubiquitin carboxyl-terminal hydrolase isozyme L3-like* and a *FKBP6-like* sequence, and could still be helping adjust to thermal stress.

GO over-representation analysis

To gain a broad understanding of the nature of changes between our samples, we tested differentially expressed genes at given temperatures as our test sets, relative to our reference transcriptomes, and checked for over-representation of any gene categories using Fisher's Exact Test, correcting for false discovery rate and with a cutoff p value of 0.05, as integrated in Blast2GO. When we compared our control to our 3 and 5 °C samples a variety of statistically significant differences in contig expression were observed (Fig 4A,B). However, there was no difference in significant GO category expression between our 3 and 5 °C samples, and we infer that this is due to only minor changes between 3 and 5 °C. These contigs change little in expression, as they are either “on” or “off” as a result of heat stress (to a degree which may or may not be significant vs the control), but cannot be modulated any further under additional stress.

In our control vs 3 °C samples (Fig 4A), GO category representation changed significantly in a number of categories. Among the GO categories downregulated at 3 °C, ‘immune response’, ‘signal transduction’ ‘serine type endopeptidase inhibitor activity’ and ‘pantothenate biosynthetic pathway’ were significantly more prevalent there than in our overall set. These GO terms indicate that immune responses and normal bodily maintenance may be perturbed by thermal stress. In contrast, GO terms associated with ribosomes and structural molecules are under-represented in this set, and therefore contigs coding for these are not present in the downregulated complement after heat exposure. This is similar to the results observed in Guzman and Conaco2016[37], as discussed further below.

In the GO categories upregulated at 3 °C, it again seems that normal metabolism is less important for response to thermal stress than cytoskeletal responses and growth factor activity. Many GO terms related to metabolic activity (e.g. ‘phosphate-containing compound metabolic process’, ‘organic substance biosynthetic process’) are under-represented in these genes relative to our overall library, while GO terms linked to microtubules and other cytoskeletal components are significantly over-represented. Taken in concert with our GO term distribution

bioRxiv preprint doi: https://doi.org/10.1101/416677; this version posted September 13, 2018. The copyright holder for this preprint (which was not certified by peer review) is the author/funder, who has granted bioRxiv a license to display the preprint in perpetuity. It is made available under aCC-BY-NC-ND 4.0 International license.

findings from downregulated genes, it seems that structural componentry is significantly upregulated in response to a 3 °C heat shock.

Many of these findings are mirrored in our control vs 5 °C samples (Fig 4B). Four GO categories, 'intracellular non-membrane-bounded organelle', 'cytoplasmic part', 'pantothenate biosynthetic process' and 'signal transduction', had similar changes in abundance in downregulated contigs from our 3 and 5 °C treatments compared to the control, and 'growth factor activity' was significantly over-represented in contigs upregulated in response to increased temperature in both samples. These have been underlined in the figure. A small number of additional categories were significantly changed in our 5 °C treatment but not observed in our 3 °C treatment, including a number of categories related to the biosynthesis of specific molecular and cellular components. For instance, the category 'cellular macromolecule biosynthetic process', is less prevalent in downregulated genes, (and therefore not itself present in downregulated contigs), while 'tyrosine biosynthetic process' and other categories are over-represented in up-regulated genes, reflecting underlying transcriptional activity in that regard, mirroring our findings in the 3 °C treatment.

Previous work [37] observed the upregulation of a number of protective and signalling-related pathways after heat shock. We see a similar pattern in our data, but the exact categories are not seen in *Isodictya* as in their warm-water *Haliclona tubifera.* Protective mechanisms in common with their results include those linked to antioxidant activity and immune response activation, but do not include the toll-like receptor (TLR) signaling pathway. We also observe similar broad representation of cellular ion homeostasis, messenger-mediated pathways, transporter activity and microtubule-based movement-linked categories, but do not see specifically calcium-mediated signaling categories, unlike those seen in their data.

While most of the observed categories in our data are quite broad and reflect changes in a number of gene families, we can observe some quite specific changes in expression. For example, the 'Tumor necrosis factor receptor binding' category is over-represented in downregulated contigs at 5 °C, suggesting that this gene family is not utilised as prevalently after heat shock. This finding was born out by our analysis of discrete contig up- and down-regulation, as discussed in detail elsewhere in this manuscript.

Identification of Target Signalling Cascades

Given the large number of un-annotatable, novel contigs in the top 20-most differentially expressed complement, we also adopted a target gene approach. From the lists of differentially expressed genes, we have selected genes previously identified as playing a role in thermal

bioRxiv preprint doi: https://doi.org/10.1101/416677; this version posted September 13, 2018. The copyright holder for this preprint (which was not certified by peer review) is the author/funder, who has granted bioRxiv a license to display the preprint in perpetuity. It is made available under aCC-BY-NC-ND 4.0 International license.

response for further study, as well as transcription factors with potential roles as cellular mediators of this process, as can be seen in Table 4. Full details of the exact expression levels of all these genes can be found in Supplementary File 4.

Heat shock proteins (HSPs) were prevalent in these complements. We obtained 4 contigs encoding a full-length sequence, corresponding to four isoforms of the gene encoding for HSP70 and related proteins. These four sequences were designed as A1, A2, B and HSP-er (contigs: TRINITY_DN27082_c0_g1, TRINITY_DN12545_c0_g2, TRINITY_DN24395_c0_g1, and TRINITY_DN20850_c0_g1_i1, respectively). The alignment of these four putative HSP70 sequences from *Isodictya* sp. alongside those previously described in sponges and other marine invertebrates, as well as related species, can be seen in Fig 5A (Full sequences, along with alignment, Supplementary File 6).

The full-length sequence of these proteins showed the presence of three classical signature motifs of the HSP70 family (IDLGTTYS; IIDLGGGTFDVSIL; IVLVGGSTRIPKI/VQK) and the ATP/GTP binding site (Fig 5B). These four forms of HSP70 in *Isodictya* possess relatively low sequence similarity (between 41.4% and 68.1% amino acid identity), and individual isoforms are more closely related to some previously described forms, which may indicate that HSP70A and B are ancestrally shared paralogues within the Porifera (Fig 5A). The HSP70A1 and 2 genes are most closely related to the non-inducible or HSP70 cognate (HSC) described for others invertebrates and vertebrates (Fig 5, Supplementary File 7). Their C-terminal region contains five repeats of GGMP motif. The tetrapeptide motif GGMP repeats are thought to be involved in co-chaperone-binding activities of constitutive forms[68]. HSP-A sequences have a terminal motif (EEVD) indicating their cytoplasmatic localisation[69]. We do not observe a clear mitochondrial-located HSP70 homologue, but HSP-er shows clear homology to known endoplasmic reticulum isoforms, and clear sequence similarity to those from both vertebrate and invertebrate species (Fig 5B).

In contrast, the isoform HSP70B showed high sequence similarity to the HSP70 sequence of *Xestospongia testudinaria* (75.4%) and this sequence does not possess tetrapeptide repeat sequences at the C-terminal (Fig 5B). HSP-B is therefore likely the "inducible" HSP gene in this species. It was up-regulated during thermal stress in this experiment, listed among the most strongly-changed in expression (Table 3), and thus shares characteristics of inducible isoforms previously described in other marine invertebrates such as oysters (see [70]).

In other species, the transcription of HSPs is upregulated in response to a variety of stresses[71], preventing the mis-folding and aggregation of proteins, but is notably absent in some

bioRxiv preprint doi: https://doi.org/10.1101/416677; this version posted September 13, 2018. The copyright holder for this preprint (which was not certified by peer review) is the author/funder, who has granted bioRxiv a license to display the preprint in perpetuity. It is made available under aCC-BY-NC-ND 4.0 International license.

species of Antarctic fish where HSPs are constitutively turned on in some cases[67]. HSPs however play a clear role in temperature response in Antarctic invertebrates [17,28,29]. Given the upregulation of isoform B here, it is clear that this role is conserved in sponges, and this collaborates findings previously in this phylum[37,72].

A number of contigs with sequence similarity to the *Tumor necrosis factor* gene family were observed in our dataset, in both our upregulated and downregulated complements (n.b. different contigs were present in the two complements). This finding dovetails with the observation of this in the GO term over-representation analysis for contigs downregulated in our 5 °C treatment. This cytokine family is responsible for regulating cell death through ubiquitins, but also has other functions, including the regulation of cell survival, proliferation and differentiation[73,74] and the downregulation of some members of this class and upregulation of others likely reflects changing cellular processes within our sponge samples of interest to those studying the molecular processes underlying thermal stress responses. A single gene linked to this has previously been observed to be upregulated after heat shock in sponges (*TNFAIP3*[37]) and the additional sequences observed here confirm the likely role of these genes in linking with ubiquitins and mediating cell death and protein degradation in Porifera after heat exposure.

The ubiquitin related genes themselves, which play essential roles in protein degradation [75,76], were well recovered in our transcriptome. Fig. 6 shows our annotation of the proteolytic pathway mediated by these genes, as annotated by bi-directional best blast hit. Of genes that are missing, few (12) may be truly absent from our transcriptomic resource- others are also absent from *A. queenslandica* and may be absent ancestrally. Three components of this pathway, TRINITY_DN31115_c0_g1 (*UBE2M; UBC12; ubiquitin-conjugating enzyme E2 M)*, TRINITY_DN8356_c0_g2 (*UBC1; ubiquitin-conjugating enzyme,* aka *HIP2; huntingtin interacting protein 2)*) and TRINITY_DN25219_c0_g1 (*UBE3A; E6AP; ubiquitin-protein ligase E3A*) were significantly upregulated in our dataset in response to heat exposure. These genes, representing E2 and HECT E3 type ubiquitin conjugating genes could play specific roles in the degeneration of misfolded and degenerated peptides after heat exposure, correlates well with previous findings in other sponge species such as *Haliclona tubifera*[37] and the specific genes are worth further consideration as potential mediators of this intracellular protective response.

We found a number of notable transcription factor and cell signalling pathways in our up- and down-regulated cassettes, including genes in the Notch, Wnt, TNF, Sox and TGF-β pathways, and have targeted these particularly for independent verification by qRT-PCR, as detailed later in this manuscript. These genes do not need to be the most up-/down-regulated

bioRxiv preprint doi: https://doi.org/10.1101/416677; this version posted September 13, 2018. The copyright holder for this preprint (which was not certified by peer review) is the author/funder, who has granted bioRxiv a license to display the preprint in perpetuity. It is made available under aCC-BY-NC-ND 4.0 International license.

genes to have a noted effect on transcription, and they represent intriguing targets as possible controllers of wider processes of molecular adaptation.

In the most similar study to this work previously performed, in the warm water sponge *H. tubifera* from Philippines[37], multiple *G protein coupled receptors* (GPCRs) were noted as differentially expressed. These genes are posited to allow these sponges to monitor and respond to their environment effectively. Several families of GPCR were noted as effected by heat exposure in *H. tubifera,* including *glutamate*, *rhodopsin* and *secretin GPCRs*. None of these were observed here, and therefore the light and contraction responses seen in *H. tubifera* on exposure to heat stress do not seem to be conserved in *Isodictya* sp. Instead, two families of orphan GPCR, *157* and *161*, were noted in our sample. The roles of these specific GPCR in sponges, and in general outside the Chordata, are poorly understood, but their marked up-regulation here, and the absence of the plethora of differentially expressed GPCR seen in *H. tubifera,* suggests that these explicit genes may play specific roles in sensing or recovering from heat exposure in this particular species.

Other examples of key cell signalling molecules identified in our study include members of the Sox and Wnt gene families, notably *Sox2* and *dishevelled*. These are possibly key in the control of growth response to heat stress - *Sox2* in particular is known for its role in the control of pluripotency in stem cell lineages[77]. Growth will both be promoted by higher temperatures, but also necessary for repairing tissue damage caused by exposure to deleterious conditions. However, by far the most commonly observed family of cell signalling molecules are representatives of the BMP/TGF-β pathway. A variety of contigs with blast similarity to the TGF-β family of signalling molecules were observed in our differentially expressed complements, including a variety of contigs annotated as bone morphogenic proteins and growth differentiation factors, as well as *one eyed pinhead* and the *Tolloid metalloprotease*, which act to modulate TGF-β signalling. These molecules are well known as modulators of cell fates, but any role in controlling response to thermal stress has not before been noted in sponges. It is possible that these molecules are acting downstream of HSP70 (as noted by Lee et al.[78]) or as part of the control of molecular response to physical damage caused by high temperatures [79]. However, the phylogenetic distance between the organisms where this has been studied and sponges is vast, and more targeted analysis is necessary to discern the true roles of these crucial molecules in this Phylum.

We noted the presence of the Hedgehog family of genes in our dataset, with both *hedgehog precursor* (TRINITY_DN46355_c0_g1_i1) and *indian hedgehog* (TRINITY_DN16789_c0_g1_i1) automatically annotated – the latter will be a slight error, as

bioRxiv preprint doi: https://doi.org/10.1101/416677; this version posted September 13, 2018. The copyright holder for this preprint (which was not certified by peer review) is the author/funder, who has granted bioRxiv a license to display the preprint in perpetuity. It is made available under aCC-BY-NC-ND 4.0 International license.

indian hedgehog is a chordate novelty generated by duplication into paralogues, and the name of this gene's annotation will derive from sequence similarity. Both contigs are therefore likely to represent variants of the *hedgehog* gene itself. These could perform key roles in the regulation of response to thermal stress, as they are instrumental in the fine-tuning of cell differentiation responses [80]. We also note the presence of members of the Notch signalling cascade in the differentially expressed complements following heat stress (e.g.TRINITY_DN30424_c0_g1_i1 *delta and Notch-like epidermal growth factor-related receptor-like*), with Notch-related contigs downregulated after exposure to both 3 and 5 °C treatments. This likely reflects changes in how cell differentiation is occurring. *Hedgehog* is often noted as a promoter of stem cell proliferation, and the initial stages of heat stress response may involve this, in concert with genes such as *Sox2* as noted above.

Marine polar organisms are interesting models for studies on the noxious effects of reactive oxygen species (ROS) in cold waters. In order to cope with the formation of deleterious ROS, some Antarctic marine invertebrates express enzymes and low-molecular weight 'scavengers' [81]. The accumulation of ROS during heat stress has been shown in previous studies on Antarctic marine species [82,83], and are important to these species given the higher levels of dissolved oxygen seen in cooler Antarctic waters. In our study, we have obtained a good sequence coverage for several enzymes implicated in antioxidant defense (Supplementary File 8). Two kinds of *superoxide dismutase* (SOD), each with different isoformal variants, were identified in *Isodictya* sp. which are differentiated by the type of metal associated with its active site of the enzyme: two contigs for *manganese SOD* (TRINITY_DN32241_c0_g1_i1 and TRINITY_DN3280_c0_g2_i1) and four contigs for a *copper/zinc SOD* (TRINITY_DN22531_ c0_g1_i1; TRINITY_DN17486_c0_g1_i1; TRINITY_DN_65_c0_g1_i1; TRINITY_DN35772 _c0_g1_i1). The SOD enzyme catalyze the first reaction in the dismutation of superoxide anions to water and hydrogen peroxide, before the catalase enzyme transforms the hydrogen peroxide into water. This enzyme is represented by three contigs that share high sequence identities with marine invertebrates such as molluscs (TRINITY_DN_6504; 28381; 29099). Another transcript well represented in our dataset was the *glutathione S-transferase* (*GST*) which plays a key role in the detoxification of ROS and the regulation of redox balance[84]. In *Isodictya* sp. seven contigs were identified with high sequence similarity to *GST*s. Previous studies have highlighted the upregulation of oxidative response and antioxidant genes in response to thermal challenge in sponges, as also observed in corals[85]. In our data, we observe the upregulation of several contigs with strong similarity to genes with antioxidant activity, *glutaredoxin* (TRINITY_DN32811_c0_g1_i1) and *thioredoxin*

bioRxiv preprint doi: https://doi.org/10.1101/416677; this version posted September 13, 2018. The copyright holder for this preprint (which was not certified by peer review) is the author/funder, who has granted bioRxiv a license to display the preprint in perpetuity. It is made available under aCC-BY-NC-ND 4.0 International license.

(TRINITY_DN32811_c0_g1_i3) [37]. The overexpression of these two small redox enzymes might be an effective mechanism in defense against oxidative stress, rather than the synthesis of larger enzymes like *catalase*, *SOD*, and *GSTs*. We also see a contig upregulated with similarity to *oxidative stress-induced growth inhibitor 2-like* (TRINITY_DN30012_c0_g1_i1), which could play a role in downstream organisation after the detection of an oxidative stress state. It seems likely that these sponges are under severe oxidative stress, and the expression of these genes reflects this.

The presence of *allograft inflammatory factor* (TRINITY DN_12683_c0_g1_i1) in our datasets was noted as these have been previously studied in Antarctic species such as the sea urchin *Sterechinus neumayeri*[86]. The deduced amino acid sequence for this contig is composed of 144 aa with a molecular weight of 16.76 KDa and an isoelectric point of 5.06. The *Isodictya* AIF-1 sequence has a high sequence similarity with that known from the sponge *Suberites domuncula,* and has two conserved calcium binding motifs known as EF hands (Fig 7). AIF-1 sequences from several invertebrate and vertebrate species were aligned and showed relatively high levels of conservation of the protein with both groups. Phylogenetic analyses generated a congruent tree positioning the AIF from sponges in a cluster with corals, distinct from vertebrate sequences. In general, *allograft inflammatory factor* is known for its role in recovery from injury, rather than any specific role in protecting against heat shock[87]. It has been studied in sponges previously[88], where it has been shown to act to activate immunocyte-like activity, as well as in protection immediately after trauma, a role which has also been noted in mammalian models. In the Japanese oyster *Crassostrea gigas* AIF-1 stimulates hemocyte immune activation by enhancing phagocytosis and expression of inflammatory cytokines[89]. Its role in the thermal stress response might therefore be in protection against infection, rather than directly in tissue repair, but both these processes are undoubtedly necessary under prolonged periods of acute thermal stress.

Proper functional dissection of the roles of these genes in these sponges is, however, beyond the scope of this manuscript, although these present excellent targets for future work. That Antarctic species of sponge utilize many of the same pathways to respond to thermal stress as warmer water species is a useful if unsurprising finding. Their efficacy at moderating response to different levels of stress does however seem to be diminished, with many of these genes expressed at both 3 and 5 °C, with no significant difference in their expression levels between these temperatures, as noted elsewhere in this work.

Poriferan Responses to Temperature Stress

bioRxiv preprint doi: https://doi.org/10.1101/416677; this version posted September 13, 2018. The copyright holder for this preprint (which was not certified by peer review) is the author/funder, who has granted bioRxiv a license to display the preprint in perpetuity. It is made available under aCC-BY-NC-ND 4.0 International license.

Our results, when considered alongside previous findings in sponges from other latitudes, corroborate previous conclusions regarding their transcriptomic response to acute thermal stress, while suggesting specifically that cold-adapted sponges may have a limited range of tolerance to increased temperatures.

The changes in transcription which occurred in our samples after thermal exposure confirmed that a poriferan heat-response cassette can be activated by increased temperatures, and is present in this species. The complements of all 4 replicates in both conditions were very similar in both overall pattern and individual composition, with differentially regulated contigs often perturbed in common at both temperatures. Previous work on sponges from other latitudes[37,54] showed that HSP70 and ubiquitin-related genes were specifically upregulated in response to thermal stress. Our work echoes this finding, observing the activation of similar genes, such as oxidation-stress related genes. The nature of the thermal stress response therefore is broadly similar to that seen in other sponge species. What may differ in Antarctic species of sponge is the limits of tolerance.

In other sponges, the degree and type of transcriptional response is temperature-dependent, with specific genes activated at different temperatures[39], where the holobiont changes, or [37], where the sponge itself adapts its transcription). In contrast, our findings showed few significant differences in the transcriptional response of sponges at 3 and 5 °C. We also do not see changes in quite the same gene cassettes, with the absence of differentially expressed GPCR and toll-like receptor (TLR) signaling genes in our data a notable difference. While previous research has demonstrated that some Antarctic species are not able to respond to additional increases in seawater temperature, other such as *Nacella concinna* or *Laternula elliptica* showed a classic thermal stress response that can over-express heat stress chaperones during the heat response[90].

A number of differences are noted in the response of cold water sponges here, when contrasted with those of warm-water species[37]. Particularly, there does not seem to be the degree of incremental change that can be seen in the transcriptional profile of warm water species to increasing temperatures, and an “all or nothing” response is observed instead. Our results did not test whether cold-adapted sponges could, in time, adapt to sequentially higher temperatures, and this would be a useful follow-up experiment to those described here. It may be possible that with a period of acclimation, sequential rises in temperature can be met by successive rounds of molecular adaptation. However, at present we cannot speculate as to whether that is possible in this species.

bioRxiv preprint doi: https://doi.org/10.1101/416677; this version posted September 13, 2018. The copyright holder for this preprint (which was not certified by peer review) is the author/funder, who has granted bioRxiv a license to display the preprint in perpetuity. It is made available under aCC-BY-NC-ND 4.0 International license.

Conclusions

Climate change is a pressing issue globally, and will have a range of effects on organisms worldwide. While some of these effects are more obvious or better studied than others, it is some of the least-studied species which will bear the brunt of these conditions, and these will have a variety of knock-on effects, the extent of which we are yet to catalogue. Here we have studied one such species, a locally abundant sponge, highly specialised to life in Antarctic conditions. We have generated an excellent reference transcriptome, and begun to identify the molecular responses that these species will use to adjust to warmer ambient temperatures. Further, we have demonstrated the clear stress that even a modest increase in temperature over a short time frame will place on such a specialist species, and that additional increases in temperature are likely to be of great consequence.

Isodictya already exercises a full measure of transcriptomic response to ambient temperatures of 3 °C, and further acute stress at 5 °C leaves it little further "wriggle room". Whether this stress results, in the wild, in the death of these sponges, or whether, given time, they will adapt to increased temperatures, is at present uncertain. However, in the interim the results presented here will allow us to begin to understand the impact of increased temperatures on these still under-investigated, but nonetheless vital, species.

Data Availability

All data are available either as Supplementary Files published on Figshare for direct download at https://figshare.com/s/0c90ae2e0b2a0524b036 and with DOI: 10.6084/m9.figshare.7048727, or from the NCBI SRA with accession number PRJNA415418.

Animal Ethics

No animal ethics approval procedure exists for Porifera, and no permission was required to perform the experiments described in this manuscript.

Permission to Carry Out Fieldwork

The study was conducted under the permit 806/2015 granted by the Chilean Antarctic Institute (INACH).

Funding

CAC supported by CONICYT/FONDECYT /INACH/INICIACION/#11150129. NJK and AR supported by the ADAPTOMICS MSCA [IF750937] under the Horizon 2020 program.

bioRxiv preprint doi: https://doi.org/10.1101/416677; this version posted September 13, 2018. The copyright holder for this preprint (which was not certified by peer review) is the author/funder, who has granted bioRxiv a license to display the preprint in perpetuity. It is made available under aCC-BY-NC-ND 4.0 International license.

Competing Interests

The authors declare they have no competing interests.

Author Contributions

MGA, MO, AF and CAC performed wet lab experiments. NJK, MGA, AR and CAC performed computational analyses. NJK, MGA and CAC wrote the main manuscript text. All authors gave final approval for publication.

Acknowledgements

The authors thank the members of their laboratories for all their support, comradeship and scholarly input. We are also grateful to the dive team, Leslie Novoa, Juana Levihuan and INACH personnel at Yelcho Station for their help during fieldwork activities in Antarctica. Cristian Lagger provided the underwater photograph of *Isodictya* sp. We thank the editors and reviewers for their aid in assessing this manuscript. This work was supported by CONICYT/FONDECYT/INACH/INICIACION/#11150129. The work of NJK was made possible by the ADAPTOMICS MSCA [IF750937] under the Horizon 2020 program. This paper contributes to the SCAR Antarctic Thresholds - Ecosystem Resilience and Adaptation (Ant-ERA) programme.

References

1. Bell JJ. The functional roles of marine sponges. Estuar Coast Shelf Sci. 2008 ;79 :341-353.

2. De Goeij JM, Van Oevelen D, Vermeij MJ, Osinga R, Middelburg JJ, de Goeij AF & Admiraal W. Surviving in a marine desert: the sponge loop retains resources within coral reefs. Science. 2013 ;342 :108-110.

3. McClintock JB, Amsler CD, Baker BJ & van Soest RWM. Ecology of Antarctic marine sponges: an overview. Int Comp Biol. 2005;45, 359-368.

4. Cárdenas CA et al. Sponge richness on algae-dominated rocky reefs in the Western Antarctic Peninsula and the Magellan Strait. Polar Res. 2016 ;35, 30532.

5. Cárdenas CA & Montiel A. Coexistence in Cold Waters: Animal Forests in Seaweed-Dominated Habitats in Southern High Latitudes in Marine Animal Forests: The Ecology of Benthic Biodiversity Hotspots (ed. Rossi S., Bramanti L., Gori A. & Orejas C.) 1-20 (Springer, 2017).

bioRxiv preprint doi: https://doi.org/10.1101/416677; this version posted September 13, 2018. The copyright holder for this preprint (which was not certified by peer review) is the author/funder, who has granted bioRxiv a license to display the preprint in perpetuity. It is made available under aCC-BY-NC-ND 4.0 International license.

6. Gutt J et al. Antarctic marine animal forests: three-dimensional communities in Southern Ocean ecosystems. Marine Animal Forests: The Ecology of Benthic Biodiversity Hotspots (ed Rossi S, Bramanti L, Gori A & Orejas C.) 1-29 (Springer, 2017).

7. Bell JJ et al. Global conservation status of sponges. Cons Biol. 2015;29,42–53.

8. Carballo JL & Bell JJ. Climate Change and Sponges: An Introduction in Climate Change, Ocean Acidification and Sponges (ed. Carballo JL & Bell JJ) 1-10 (Springer, 2017)

9. Meredith MP & King JC. Rapid climate change in the ocean west of the Antarctic Peninsula during the second half of the 20th century. Geophys Res Lett. 2005;32, 19604–19609.

10. Stenni B, et al. Antarctic climate variability on regional and continental scales over the last 2000 years. Climate of the Past. 2017;13, 1609-1634.

11. IPCC Climate Change 2014: Impacts, Adaptation, and Vulnerability in Intergovernmental Panel on Climate Change. Working Group II Report (IPCC, 2014).

12. Peck L, Morley S & Clark M. Poor acclimation capacities in Antarctic marine ectotherms. Mar Biol. 2010;157, 2051-2059.

13. Ingels J et al. Possible effects of global environmental changes on Antarctic benthos: a synthesis across five major taxa. Ecol Evol. 2012;2, 453-485.

14. Berg MP et al. Adapt or disperse: understanding species persistence in a changing world. Glob Change Biol. 2010;16, 587-98.

15. Peck L, Morley S, Richard J & Clark M. Acclimation and thermal tolerance in Antarctic marine ectotherms. J Exp Biol. 2014;217, 16-22.

16. Suckling CC et al. Adult acclimation to combined temperature and pH stressors significantly enhances reproductive outcomes compared to short-term exposures. J Anim Ecol. 2015;84, 773-784.

17. Clark MS et al. Biodiversity in marine invertebrate responses to acute warming revealed by a comparative multi-omics approach. Glob Change Biol. 2017;23: 318-330.

18. Ramsby BD, Hoogenboom MO, Smith H A, Whalan S & Webster NS. The bioeroding sponge *Cliona orientalis* will not tolerate future projected ocean warming. Sci Rep. 2018;8, 8302.

19. Duckworth AR, West L, Vansach T, Stubler A & Hardt M. Effects of water temperature and pH on growth and metabolite biosynthesis of coral reef sponges. Mar Ecol Prog Ser. 2012;462, 67–77.

20. Kelmo F, Bell JJ & Attrill MJ. Tolerance of sponge assemblages to temperature anomalies: resilience and proliferation of sponges following the 1997–8 El-Nino southern oscillation. 2013;PLoS ONE. 8, e76441.

bioRxiv preprint doi: https://doi.org/10.1101/416677; this version posted September 13, 2018. The copyright holder for this preprint (which was not certified by peer review) is the author/funder, who has granted bioRxiv a license to display the preprint in perpetuity. It is made available under aCC-BY-NC-ND 4.0 International license.

21. Strand R et al. The response of a boreal deep-sea sponge holobiont to acute thermal stress. Sci Rep. 2017;7, 1660.

22. Cebrian E, Uriz MJ, Garrabou J & Ballesteros E. Sponge mass mortalities in a warming Mediterranean Sea: are cyanobacteria-harboring species worse off?. PLoS One. 2011;6, 20211.

23. Webster N et al. A complex life cycle in a warming planet: gene expression in thermally stressed sponges. Mol Ecol. 2013;22, 1854–1868.

24. Ettinger-Epstein P, Whalan S, Battershill CN & de Nys R. Temperature cues gametogenesis and larval release in a tropical sponge. Mar Biol. 2007;153,171–178.

25. Massaro AJ, Weisz JB, Hill MS & Webster NS. Behavioral and morphological changes caused by thermal stress in the great barrier reef sponge *Rhopaloeides odorabile*. J Exp Mar Biol Ecol. 2012;417, 55–60.

26. Cerrano C et al. A catastrophic mass-mortality episode of gorgonians and other organisms in the Ligurian Sea (North-western Mediterranean), summer 1999. Ecol Lett. 2000;3, 284-293.

27. Peck LS. Prospects for survival in the Southern Ocean: vulnerability of benthic species to temperature change. Antarct Sci. 2005;17, 497-507.

28. Clark MS et al. Insights into shell deposition in the Antarctic bivalve *Laternula elliptica*: gene discovery in the mantle transcriptome using 454 pyrosequencing. BMC Genom. 2010;11, 362.

29. Johnson KM & Hofmann GE. A transcriptome resource for the Antarctic pteropod *Limacina helicina antarctica*. Mar Genom. 2016;28, 25-28.

30. Klinck JM, Hofmann EE, Beardsley RC, Salihoglu B & Howard S. Water-mass properties and circulation on the west Antarctic Peninsula Continental Shelf in Austral Fall and Winter 2001. Deep Sea Res II: Topical Studies in Oceanography, 51, 1925-1946 (2004).

31. Cárdenas CA, González-Aravena M & Santibañez PA. The importance of local settings: within-year variability in seawater temperature at South Bay, Western Antarctic Peninsula. PeerJ. 2018;6, e4289.

32. Cahais V et al. Reference-free transcriptome assembly in non-model animals from next-generation sequencing data. Mol Ecol Resources. 2012;12, 834-845.

33. Goodwin S, McPherson JD & McCombie WR. Coming of age: ten years of next-generation sequencing technologies. Nat Rev Genet. 2016;17, 333-351.

34. Pérez-Porro AR, Navarro-Gómez D, Uriz MJ & Giribet, G. A NGS approach to the encrusting Mediterranean sponge *Crella elegans* (Porifera, Demospongiae, Poecilosclerida): transcriptome sequencing, characterization and overview of the gene expression along three life cycle stages. Mol Ecol Res. 2013;13, 494-509.

bioRxiv preprint doi: https://doi.org/10.1101/416677; this version posted September 13, 2018. The copyright holder for this preprint (which was not certified by peer review) is the author/funder, who has granted bioRxiv a license to display the preprint in perpetuity. It is made available under aCC-BY-NC-ND 4.0 International license.

35. Riesgo A, Farrar N, Windsor PJ, Giribet G & Leys SP. The analysis of eight transcriptomes from all poriferan classes reveals surprising genetic complexity in sponges. Mol Biol Evol. 2014;31, 1102-1120.

36. Fernandez-Valverde SL, Calcino AD & Degnan BM. Deep developmental transcriptome sequencing uncovers numerous new genes and enhances gene annotation in the sponge Amphimedon queenslandica. BMC Genom.2015;16, 387.

37. Guzman C & Conaco C. Gene expression dynamics accompanying the sponge thermal stress response. PLoS ONE. 2016;11, e0165368.

38. Erwin PM, Pita L, Lopez-Legentil S & Turon X. Stability of sponge-associated bacteria over large seasonal shifts in temperature and irradiance. Appl Environ Microbiol. 2012;78, 7358–7368.

39. Fan L, Liu M, Simister R, Webster NS & Thomas T. Marine microbial symbiosis heats up: the phylogenetic and functional response of a sponge holobiont to thermal stress. ISME J. 2013;7, 991–1002.

40. Pita L, Turon X, Lopez-Legentil S & Erwin PM. Host rules: spatial stability of bacterial communities associated with marine sponges (Ircinia spp.) in the Western Mediterranean Sea. FEMS Microbiol Ecol. 2013;86, 268–276.

41. Simister R, Taylor MW, Tsai P & Webster N. Sponge-microbe associations survive high nutrients and temperatures. PLoS ONE. 2012;7, e52220.

42. Lopez-Legentil S, Song B, McMurray SE & Pawlik JR. Bleaching and stress in coral reef ecosystems: hsp70 expression by the giant barrel sponge *Xestospongia muta*. Mol Ecol. 2008;17, 1840–1849.

43. Andrews S. FastQC: A quality control tool for high throughput sequence data. Babraham Bioinformatics. 2010; http://www.bioinformatics.babraham.ac.uk/projects/fastqc/.

44. Bolger AM, Lohse M & Usadel B. Trimmomatic: a flexible trimmer for Illumina sequence data. Bioinformatics. 2014;30, 2114–2120.

45. Li H. Seqtk: a fast and lightweight tool for processing FASTA or FASTQ sequences, Github. 2013; https://github.com/lh3/seqtk.

46. Grabherr MG et al. Full-length transcriptome assembly from RNA-Seq data without a reference genome. Nat Biotechnol. 2011;29, 644–652.

47. Schmieder R & Edwards R. Fast identification and removal of sequence contamination from genomic and metagenomic datasets. PLoS One. 2011;6, e17288.

48. Altschul SF et al. Basic local alignment search tool. J. Mol Biol. 1990;215, 403-10.

bioRxiv preprint doi: https://doi.org/10.1101/416677; this version posted September 13, 2018. The copyright holder for this preprint (which was not certified by peer review) is the author/funder, who has granted bioRxiv a license to display the preprint in perpetuity. It is made available under aCC-BY-NC-ND 4.0 International license.

49. Katoh K & Standley DM. MAFFT multiple sequence alignment software version 7: improvements in performance and usability. Mol Biol Evol. 2013;30, 772-780.

50. Castresana J. Selection of conserved blocks from multiple alignments for their use in phylogenetic analysis. Mol Biol Evol. 2000;17, 540-552.

51. Silvestro, M. raxmlGUI: a graphical front-end for RAxML. Organis Div Evol. 2012;12, 335-337.

52. Kumar S, Stecher G & Tamura K. MEGA7: molecular evolutionary genetics analysis version 7.0 for bigger datasets. Mol Biol Evol. 2016;33, 1870-1874.

53. Larkin MA et al. Clustal W and Clustal X version 2.0. Bioinformatics. 2007;23, 2947-2948.

54. Gouy M, Guindon S & Gascuel, O. SeaView version 4: a multiplatform graphical user interface for sequence alignment and phylogenetic tree building. Mol Biol Evol. 2009;27, 221-224.

55. Simao FA, Waterhouse RM, Ioannidis P, Kriventseva EV & Zdobnov EM. BUSCO: assessing genome assembly and annotation completeness with single-copy orthologs. Bioinformatics. 2015;31, 3210–3212.

56. Conesa A et al. Blast2GO: a universal tool for annotation, visualization and analysis in functional genomics research. Bioinformatics.2005;15, 3674-3676.

57. Moriya Y, Itoh M, Okuda S, Yoshizawa AC & Kanehisa M. KAAS: an automatic genome annotation and pathway reconstruction server. Nucleic Acids Res. 2007;35, 182-185.

58. Li B & Dewey CN. RSEM: accurate transcript quantification from RNA-Seq data with or without a reference genome. BMC Bioinformat. 2011;12, 323.

59. Langmead B & Salzberg SL. Fast gapped-read alignment with Bowtie 2. Nat Methods. 2012;9, 357-359.

60. Robinson MD, McCarthy DJ & Smyth GK. edgeR: a Bioconductor package for differential expression analysis of digital gene expression data. Bioinformatics. 2010;1,139-140.

61. Benjamini Y & Hochberg Y. Controlling the false discovery rate: a practical and powerful approach to multiple testing. J Royal Stat Soc B. 1995;57, 289-300.

62. Hansen KD, Brenner SE & Dudoit S. Biases in Illumina transcriptome sequencing caused by random hexamer priming. Nucleic Acids Res. 2010;38, e131.

63. Woese CR, Kandler O & Wheelis ML. Towards a natural system of organisms: proposal for the domains Archaea, Bacteria, and Eucarya. PNAS USA. 1990;87, 4576-4579.

64. Kenny NJ et al. Towards the identification of ancestrally shared regenerative mechanisms across the Metazoa: a transcriptomic case study in the demosponge *Halisarca caerulea*. Mar Genom. 2018;37, 135-147.

bioRxiv preprint doi: https://doi.org/10.1101/416677; this version posted September 13, 2018. The copyright holder for this preprint (which was not certified by peer review) is the author/funder, who has granted bioRxiv a license to display the preprint in perpetuity. It is made available under aCC-BY-NC-ND 4.0 International license.

65. Cerrano C et al. Diatom invasion in the antarctic hexactinellid sponge *Scolymastra joubini*. Polar Biol. 2000;23, 441-444.

66. Cerrano C, Cucchiari E, Di Camillo C, Totti C & Bavestrello G. The diversity of relationships between Antarctic sponges and diatoms the case of *Mycale acerata* Kirkpatrick, 1907 (Porifera, Demospongiae). Polar Biol. 2004;27, 231-237.

67. Hofmann GE, Buckley BA, Airaksinen S, Keen JE & Somero GN. Heat-shock protein expression is absent in the antarctic fish *Trematomus bernacchii* (family Nototheniidae). J Exp Biol. 2000;203, 2331-2339.

68. Cascella K et al. Diversification, Evolution and Sub-Functionalization of 70kDa Heat- Shock Proteins in Two Sister Species of Antarctic Krill: Differences in Thermal Habitats, Responses and Implications under Climate Change. PLoS ONE. 2015;10, 0121642.

69. Shonhai A, Boshoff A & Blatch GL. The structural and functional diversity of Hsp70 proteins from *Plasmodium falciparum*. Prot Sci, 2007;16(9), 1803–1818.

70. Piano A, Franzellitti S, Tinti F & Fabbri E. Sequencing and expression pattern of inducible heat shock gene products in the European flat oyster, *Ostrea edulis*. Gene. 2005;361, 119–126.

71. Craig EA & Gross CA. Is hsp70 the cellular thermometer?. Trends Biochem Sci. 1991;16,135-140.

72. Krasko A et al. Diagnosis of sublethal stress in the marine sponge *Geodia cydonium*: application of the 70 kDa heat-shock protein and a novel biomarker, the Rab GDP dissociation inhibitor, as probes. Aquat Toxicol. 1997;37,157-168.

73. Vilcek J & Lee TH. Tumor necrosis factor. New insights into the molecular mechanisms of its multiple actions. J Biol Chem. 1991;266, .7313-7316.

74. Wang X & Lin Y. Tumor necrosis factor and cancer, buddies or foes?. Acta Pharmacologica Sinica. 2008;29, 1275-1288.

75. Glickman MH & Ciechanover A. The ubiquitin-proteasome proteolytic pathway: destruction for the sake of construction. Physiol Rev. 2002;82, 373-428.

76. Mukhopadhyay D & Riezman H. Proteasome-independent functions of ubiquitin in endocytosis and signaling. Science. 2007;315, 201-205.

77. Rizzino A. Sox2 and Oct 3/4: a versatile pair of master regulators that orchestrate the self-renewal and pluripotency of embryonic stem cells. WIREs Syst Biol Med. 2009;1, 228-236.

78. Yao Y, Watson AD, Ji S & Boström KI. Heat shock protein 70 enhances vascular bone morphogenetic protein-4 signaling by binding matrix Gla protein. Circulation Res. 2009;105, 575-584.

bioRxiv preprint doi: https://doi.org/10.1101/416677; this version posted September 13, 2018. The copyright holder for this preprint (which was not certified by peer review) is the author/funder, who has granted bioRxiv a license to display the preprint in perpetuity. It is made available under aCC-BY-NC-ND 4.0 International license.

79. Lee SB, Lim AR, Rah DK, Kim KS & Min HJ. Modulation of heat shock protein 90 affects TGF-β-induced collagen synthesis in human dermal fibroblast cells. Tiss Cell. 2016;48, 616-623.

80. Ingham PW & McMahon AP. Hedgehog signaling in animal development: paradigms and principles. Genes Dev. 2001;15, 3059-3087.

81. Camus L, Gulliksen B, Depledge M H & Jones M B. Polar bivalves are characterized by high antioxidant defences. Polar Res. 2005;24,1-2.

82. Abele D, Burlando B, Viarengo A & Pörtner HO. Exposure to elevated temperatures and hydrogen peroxide elicits oxidative stress and antioxidant response in the Antarctic intertidal limpet *Nacella concinna*. Comp Biochem Physiol B. 1998;120, 425-435.

83. Heise K, Puntarulo S, Portner HO & Abele D. Production of reactive oxygen species by isolated mitochondria of the Antarctic bivalve *Laternula elliptica* (King and Broderip) under heat stress. Comp Biochem Physiol C. 2003;134, 79-90.

84. Kim M, Ahn IY, Cheon J & Park H. Molecular cloning and thermal stress-induced expression of a pi-class glutathione S-transferase (GST) in the Antarctic bivalve *Laternula elliptica*. Comp Biochem. Physiol A Mol Integr Physiol, 2009;152, 207-213.

85. DeSalvo MK et al. Differential gene expression during thermal stress and bleaching in the Caribbean coral *Montastraea faveolata*. Mol Ecol. 2008;17, 3952–3971.

86. Ovando F et al. Cloning and expression analysis of allograft inflammatory factor type 1 in coelomocytes of Antarctic sea urchin (*Sterechinus neumayeri*). J Shellfish Res. 2012;31. 875-883.

87. Utans U, Arceci RJ, Yamashita Y & Russell ME. Cloning and characterization of allograft inflammatory factor-1: a novel macrophage factor identified in rat cardiac allografts with chronic rejection. J Clinic Invest. 1995;95 2954.

88. Kruse M, Steffen R, Batel R, Muller IM & Muller WE. Differential expression of allograft inflammatory factor 1 and of glutathione peroxidase during auto-and allograft response in marine sponges. J Cell Sci. 1999;112, 4305-4313.

89. Zhang Y, Li J, Yu F, He X & Yu Z. Allograft inflammatory factor-1 stimulates hemocyte immune activation by enhancing phagocytosis and expression of inflammatory cytokines in *Crassostrea gigas*. Fish Shellfish Immunol. 2013;34, 1071-1077.

90. Peck LS. A Cold Limit to Adaptation in the Sea. Trends Ecol Evol. 2016;31, 13-26.

bioRxiv preprint doi: https://doi.org/10.1101/416677; this version posted September 13, 2018. The copyright holder for this preprint (which was not certified by peer review) is the author/funder, who has granted bioRxiv a license to display the preprint in perpetuity. It is made available under aCC-BY-NC-ND 4.0 International license.

Tables

Table 1: Raw Read Data, Before and After Cleaning

Metric	Control (209)	3 °C Replicate A (117)	3 °C Replicate B (123)	5 °C Replicate A (135)	5 °C Replicate B (141)
Total Read Pairs (Initial)	25,988,569	28,513,364	26,960,296	25,793,570	26,289,401
Total Read Pairs (After Cleaning)	18,784,882	20,653,864	19,553,789	18,122,106	18,763,103
Total Bases in All Reads (Initial)	5,249,690,938	5,759,699,528	5,445,979,792	5,210,301,140	5,310,459,002
Total Bases in All Reads (After Cleaning)	3,591,119,834	3,940,343,972	3,742,325,651	3,441,581,533	3,575,958,067
GC% (Initial)	45	46	45	46	45
GC% (After Cleaning)	45	46	44	46	44
Average Q (Initial)	35.75	35.75	35.8	35.55	35.75
Average Q (After Cleaning)	37.45	37.4	37.45	37.4	37.4
% less than Q20 (Initial)	4.55	4.55	4.55	5.05	4.7
% less than Q20 (After Cleaning)	0.2	0.2	0.2	0.25	0.25

bioRxiv preprint doi: https://doi.org/10.1101/416677; this version posted September 13, 2018. The copyright holder for this preprint (which was not certified by peer review) is the author/funder, who has granted bioRxiv a license to display the preprint in perpetuity. It is made available under aCC-BY-NC-ND 4.0 International license.

Table 2: Statistics, Reference Transcriptome Assembly

Number of transcripts	90,188
Number of Trinity 'genes'	70,844
Total bp in assembly	59,274,448
Max contig length (bp)	19,068
Mean contig length (bp)	657.23
Median contig length (bp)	338
% GC	43.10 %
N20 Contig Length	2,921
N50 Contig Length	1,113
# contigs in N50	12,997
Number of transcripts over 1000 bp	14,633
Transcripts w/ blast hit	20,607
Transcripts w/ GO term	12,924

bioRxiv preprint doi: https://doi.org/10.1101/416677; this version posted September 13, 2018. The copyright holder for this preprint (which was not certified by peer review) is the author/funder, who has granted bioRxiv a license to display the preprint in perpetuity. It is made available under aCC-BY-NC-ND 4.0 International license.

Table 3: The 20 most up/downregulated contigs in each sample cross-comparison

20 Most Differentially Expressed Genes					
Control vs 3 degrees, Downregulated	**Annotation**	**Control vs 5 degrees, downregulated**	**Annotation**	**3 vs 5 degrees, downregulated**	**Annotation**
TRINITY_DN20177_c1_g1	---NA---	TRINITY_DN24223_c2_g2	PLANT CADMIUM RESISTANCE 3-like	TRINITY_DN23764_c0_g2	polyadenylate-binding -interacting 1-like
TRINITY_DN33508_c0_g1	---NA---	TRINITY_DN20177_c1_g1	---NA---	TRINITY_DN24223_c2_g2	PLANT CADMIUM RESISTANCE 3-like
TRINITY_DN45390_c0_g1	---NA---	TRINITY_DN8570_c0_g1	hypothetical protein	TRINITY_DN12683_c0_g1	allograft inflammatory factor 1
TRINITY_DN33508_c0_g4	---NA---	TRINITY_DN32712_c4_g3	---NA---	TRINITY_DN6163_c0_g2	ubiquitin carboxyl-terminal hydrolase isozyme L3-like
TRINITY_DN35469_c0_g1	soluble calcium-activated nucleotidase 1 isoform X1	TRINITY_DN24027_c0_g1	---NA---	TRINITY_DN23190_c0_g1	---NA---
TRINITY_DN35123_c0_g3	---NA---	TRINITY_DN40223_c0_g1	---NA---	TRINITY_DN24468_c0_g2	---NA---
TRINITY_DN19331_c1_g1	hypothetical protein	TRINITY_DN8786_c0_g1	oxysterol-binding 1-like	TRINITY_DN30615_c2_g9	---NA---
TRINITY_DN24815_c0_g1	---NA---	TRINITY_DN35469_c0_g1	soluble calcium-activated nucleotidase 1 isoform X1	TRINITY_DN8356_c0_g2	ubiquitin-conjugating enzyme E2 K-like
TRINITY_DN8271_c0_g1	---NA---	TRINITY_DN45390_c0_g1	---NA---	TRINITY_DN26078_c0_g2	COMM domain-containing 8-like
TRINITY_DN31187_c0_g1	---NA---	TRINITY_DN33246_c0_g3	---NA---	TRINITY_DN58418_c0_g1	nucleoporin GLE1-like
TRINITY_DN49200_c0_g1	---NA---	TRINITY_DN33508_c0_g4	---NA---	TRINITY_DN35203_c0_g2	---NA---
TRINITY_DN33462_c0_g1	---NA---	TRINITY_DN11747_c0_g1	hypothetical protein, partial		
TRINITY_DN4804_c0_g2	hypothetical protein TRIADDRAFT_59764	TRINITY_DN24815_c0_g1	---NA---		
TRINITY_DN23863_c0_g1	---NA---	TRINITY_DN24481_c0_g1	---NA---		
TRINITY_DN33246_c0_g3	---NA---	TRINITY_DN30570_c0_g1	replicase poly		
TRINITY_DN30570_c0_g1	---NA---	TRINITY_DN35123_c0_g3	---NA---		
TRINITY_DN26078_c0_g1	COMM domain-containing 8-like	TRINITY_DN59119_c0_g1	---NA---		
TRINITY_DN12307_c0_g1	PREDICTED: uncharacterized protein	TRINITY_DN13825_c0_g1	endoplasmic reticulum-Golgi intermediate compartment 3-like		
TRINITY_DN36675_c0_g1	---NA---	TRINITY_DN26662_c0_g1	hypothetical protein crov191		
Control vs 3 degrees, Upregulated	**Annotation**	**Control vs 5 degrees, Upregulated**	**Annotation**	**3 vs 5 degrees, upregulated**	**Annotation**
TRINITY_DN24284_c0_g3	hypothetical protein BRAFLDRAFT_114823	TRINITY_DN24284_c0_g3	hypothetical protein BRAFLDRAFT_114823	TRINITY_DN33462_c0_g1	---NA---
TRINITY_DN44573_c0_g1	hypothetical protein	TRINITY_DN24223_c2_g1	PLANT CADMIUM RESISTANCE 3-like	TRINITY_DN53922_c0_g3	inactive peptidyl-prolyl cis-trans isomerase FKBP6-like

bioRxiv preprint doi: https://doi.org/10.1101/416677; this version posted September 13, 2018. The copyright holder for this preprint (which was not certified by peer review) is the author/funder, who has granted bioRxiv a license to display the preprint in perpetuity. It is made available under aCC-BY-NC-ND 4.0 International license.

TRINITY_DN18944_c0_g2	40S ribosomal S13	TRINITY_DN44573_c0_g1	hypothetical protein	TRINITY_DN23764_c0_g1	polyadenylate-binding -interacting 1-like
TRINITY_DN33508_c0_g2	---NA---	TRINITY_DN22854_c0_g2	PREDICTED: tetraspanin-7-like	TRINITY_DN58083_c0_g1	---NA---
TRINITY_DN24223_c2_g1	PLANT CADMIUM RESISTANCE 3-like	TRINITY_DN8786_c0_g2	oxysterol-binding 1-like	TRINITY_DN23863_c0_g1	---NA---
TRINITY_DN34845_c4_g12	---NA---	TRINITY_DN29050_c0_g1	hypothetical protein		
TRINITY_DN34845_c4_g3	---NA---	TRINITY_DN18944_c0_g2	40S ribosomal S13		
TRINITY_DN22854_c0_g2	PREDICTED: tetraspanin-7-like	TRINITY_DN53805_c0_g1	PREDICTED: uncharacterized protein		
TRINITY_DN34845_c4_g9	---NA---	TRINITY_DN30712_c0_g1	---NA---		
TRINITY_DN22240_c0_g4	---NA---	TRINITY_DN58083_c0_g1	---NA---		
TRINITY_DN34845_c4_g10	---NA---	TRINITY_DN26231_c0_g4	dolichyl-diphosphooligosaccharide-- glycosyltransferase 48 kDa subunit-like		
TRINITY_DN44814_c0_g1	---NA---	TRINITY_DN27017_c0_g1	---NA---		
TRINITY_DN26511_c0_g1	hypothetical protein	TRINITY_DN34845_c4_g10	---NA---		
TRINITY_DN34845_c4_g4	---NA---	TRINITY_DN24395_c0_g1	heat shock 70 B2-like		
TRINITY_DN1002_c0_g1	predicted protein	TRINITY_DN34845_c4_g4	---NA---		
TRINITY_DN23682_c0_g2	---NA---	TRINITY_DN34845_c4_g12	---NA---		
TRINITY_DN26231_c0_g4	dolichyl-diphosphooligosaccharide-- glycosyltransferase 48 kDa subunit-like	TRINITY_DN34845_c4_g3	---NA---		
TRINITY_DN2258_c0_g1	40S ribosomal S25	TRINITY_DN22240_c0_g4	---NA---		
TRINITY_DN30873_c1_g2	---NA---	TRINITY_DN26511_c0_g1	---NA---		
TRINITY_DN20209_c0_g1	---NA---	TRINITY_DN34845_c4_g9	---NA---		

bioRxiv preprint doi: https://doi.org/10.1101/416677; this version posted September 13, 2018. The copyright holder for this preprint (which was not certified by peer review) is the author/funder, who has granted bioRxiv a license to display the preprint in perpetuity. It is made available under aCC-BY-NC-ND 4.0 International license.

Table 4: Manually identified target genes

Target gene approach					
Control vs 3 degrees, Downregulated	**Annotation**	**Control vs 5 degrees, downregulated**	**Annotation**	**3 vs 5 degrees, downregulated**	**Annotation**
TRINITY_DN49841_c0_g3_i1	tumor necrosis factor ligand superfamily member 15	TRINITY_DN49841_c0_g3_i1	tumor necrosis factor ligand superfamily member 15	TRINITY_DN23764_c0_g2	polyadenylate-binding - interacting 1-like
TRINITY_DN49577_c0_g1_i1	mesoderm development candidate 1-like	TRINITY_DN49577_c0_g1_i1	mesoderm development candidate 1-like	TRINITY_DN24223_c2_g2	PLANT CADMIUM RESISTANCE 3-like
TRINITY_DN34885_c0_g2_i2	neurogenic locus notch homolog 1-like	TRINITY_DN34885_c0_g2_i2	neurogenic locus notch homolog 1-like	TRINITY_DN12683_c0_g1	allograft inflammatory factor 1
TRINITY_DN28743_c0_g1_i1	E3 ubiquitin- ligase TRIM71-like	TRINITY_DN28743_c0_g1_i1	E3 ubiquitin- ligase TRIM71-like	TRINITY_DN6163_c0_g2	ubiquitin carboxyl-terminal hydrolase isozyme L3-like
TRINITY_DN28248_c0_g1_i1	ribosome-binding 1-like	TRINITY_DN33363_c1_g1_i1	G2 M phase-specific E3 ubiquitin- ligase- partial	TRINITY_DN8356_c0_g2	ubiquitin-conjugating enzyme E2 K-like
TRINITY_DN30424_c0_g1_i1	delta and Notch-like epidermal growth factor-related receptor-like	TRINITY_DN28248_c0_g1_i1	ribosome-binding 1-like	TRINITY_DN26078_c0_g2	COMM domain-containing 8-like
TRINITY_DN31499_c1_g3_i1	calmodulin isoform X1	TRINITY_DN4806_c0_g1_i1	polycomb group RING finger 1-like	TRINITY_DN58418_c0_g1	nucleoporin GLE1-like
TRINITY_DN29988_c0_g1_i1	TGF-beta receptor type-1-like	TRINITY_DN30424_c0_g1_i1	delta and Notch-like epidermal growth factor-related receptor-like		
TRINITY_DN35391_c8_g6_i2	TNF receptor-associated factor 5-like	TRINITY_DN31499_c1_g3_i1	calmodulin isoform X1		
TRINITY_DN29288_c0_g1_i1	G- coupled receptor 161-like	TRINITY_DN35391_c8_g6_i2	TNF receptor-associated factor 5-like		
TRINITY_DN54189_c0_g2_i1	probable G- coupled receptor 157	TRINITY_DN29288_c0_g1_i1	G- coupled receptor 161-like		
		TRINITY_DN54189_c0_g2_i1	probable G- coupled receptor 157		
Control vs 3 degrees, Upregulated	**Annotation**	**Control vs 5 degrees, Upregulated**	**Annotation**	**3 vs 5 degrees, upregulated**	**Annotation**
TRINITY_DN12683_c0_g1_i1	allograft inflammatory factor 1	TRINITY_DN25219_c0_g1_i1	ubiquitin- ligase E3A-like	TRINITY_DN53922_c0_g3	inactive peptidyl-prolyl cis-trans isomerase FKBP6-like
TRINITY_DN27456_c0_g1_i1	tolloid 1	TRINITY_DN40009_c0_g1_i1	transcription factor Sox-2-like	TRINITY_DN23764_c0_g1	polyadenylate-binding - interacting 1-like
TRINITY_DN25219_c0_g1_i1	ubiquitin- ligase E3A-like	TRINITY_DN24395_c0_g1_i1	heat shock 70 B2-like		
TRINITY_DN40009_c0_g1_i1	transcription factor Sox-2-like	TRINITY_DN33837_c0_g3_i1	TNF receptor-associated factor 5-like		
TRINITY_DN24395_c0_g1_i1	heat shock 70 B2-like	TRINITY_DN34897_c0_g1_i1	tolloid 2		
TRINITY_DN16789_c0_g1_i1	indian hedgehog	TRINITY_DN29751_c0_g1_i1	growth differentiation factor 7		
TRINITY_DN33837_c0_g3_i1	TNF receptor-associated factor 5-like	TRINITY_DN29790_c0_g3_i1	ubiquitin-60S ribosomal L40		
TRINITY_DN34897_c0_g1_i1	tolloid 2	TRINITY_DN35733_c0_g1_i1	probable E3 ubiquitin-ligase partial		

bioRxiv preprint doi: https://doi.org/10.1101/416677; this version posted September 13, 2018. The copyright holder for this preprint (which was not certified by peer review) is the author/funder, who has granted bioRxiv a license to display the preprint in perpetuity. It is made available under aCC-BY-NC-ND 4.0 International license.

TRINITY_DN29790_c0_g3_i1	ubiquitin-60S ribosomal L40	TRINITY_DN16075_c0_g1_i1	bone morphogenetic 7		
TRINITY_DN28521_c0_g1_i1	bone morphogenetic 6-like	TRINITY_DN27508_c0_g1_i1	growth differentiation factor 8-like		
TRINITY_DN8356_c0_g2_i1	ubiquitin-conjugating enzyme E2 K-like	TRINITY_DN27456_c0_g1_i1	tolloid 1		
TRINITY_DN16075_c0_g1_i1	bone morphogenetic 7	TRINITY_DN34419_c1_g1_i1	pinhead precursor		
TRINITY_DN27508_c0_g1_i1	growth differentiation factor 8-like	TRINITY_DN30012_c0_g1_i1	oxidative stress-induced growth inhibitor 2-like		
TRINITY_DN31167_c0_g1_i2	segment polarity dishevelled homolog	TRINITY_DN32735_c0_g1_i2	G- coupled receptor 161-like		
TRINITY_DN46355_c0_g1_i1	hedgehog precursor				
TRINITY_DN34419_c1_g1_i1	pinhead precursor				
TRINITY_DN19433_c0_g1_i1	MULTISPECIES: cold-shock				
TRINITY_DN32811_c0_g1_i1	glutaredoxin				
TRINITY_DN32811_c0_g1_i3	thioredoxin				
TRINITY_DN33675_c0_g2_i1	alkyl hydroperoxide reductase				

bioRxiv preprint doi: https://doi.org/10.1101/416677; this version posted September 13, 2018. The copyright holder for this preprint (which was not certified by peer review) is the author/funder, who has granted bioRxiv a license to display the preprint in perpetuity. It is made available under aCC-BY-NC-ND 4.0 International license.

Figure Legends

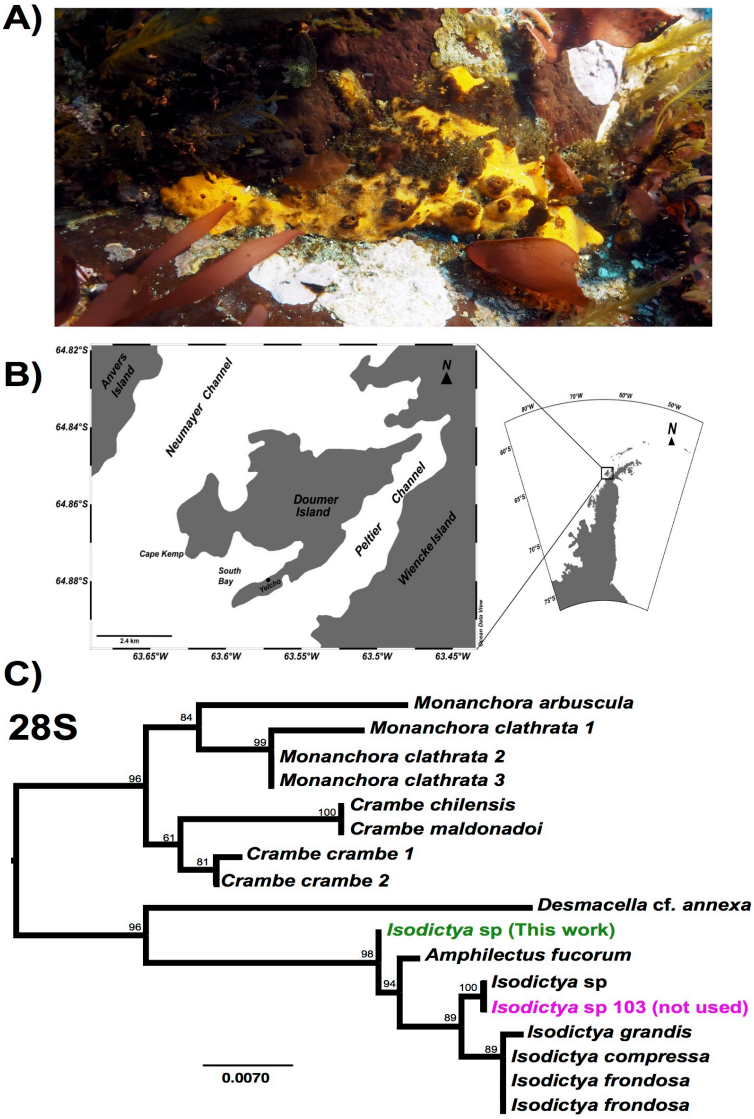

Figure 1: A) Image of *Isodictya* sp. collected at South Bay, WAP (10 m depth). B) Sample collection location, Doumer Island, WAP. C) RAxML trees of 28S rRNA under the GTR model from the *Isodictya* species mentioned in this manuscript, along with those of related species. Note the difference in placement of the samples used in the present manuscript (in green, *Isodictya* sp. (This work)) to that of one of the samples sequenced for this work, *Isodictya* sp. 103 (in magenta), which was excluded due to its being identity as a cryptic, but separate, species.

bioRxiv preprint doi: https://doi.org/10.1101/416677; this version posted September 13, 2018. The copyright holder for this preprint (which was not certified by peer review) is the author/funder, who has granted bioRxiv a license to display the preprint in perpetuity. It is made available under aCC-BY-NC-ND 4.0 International license.

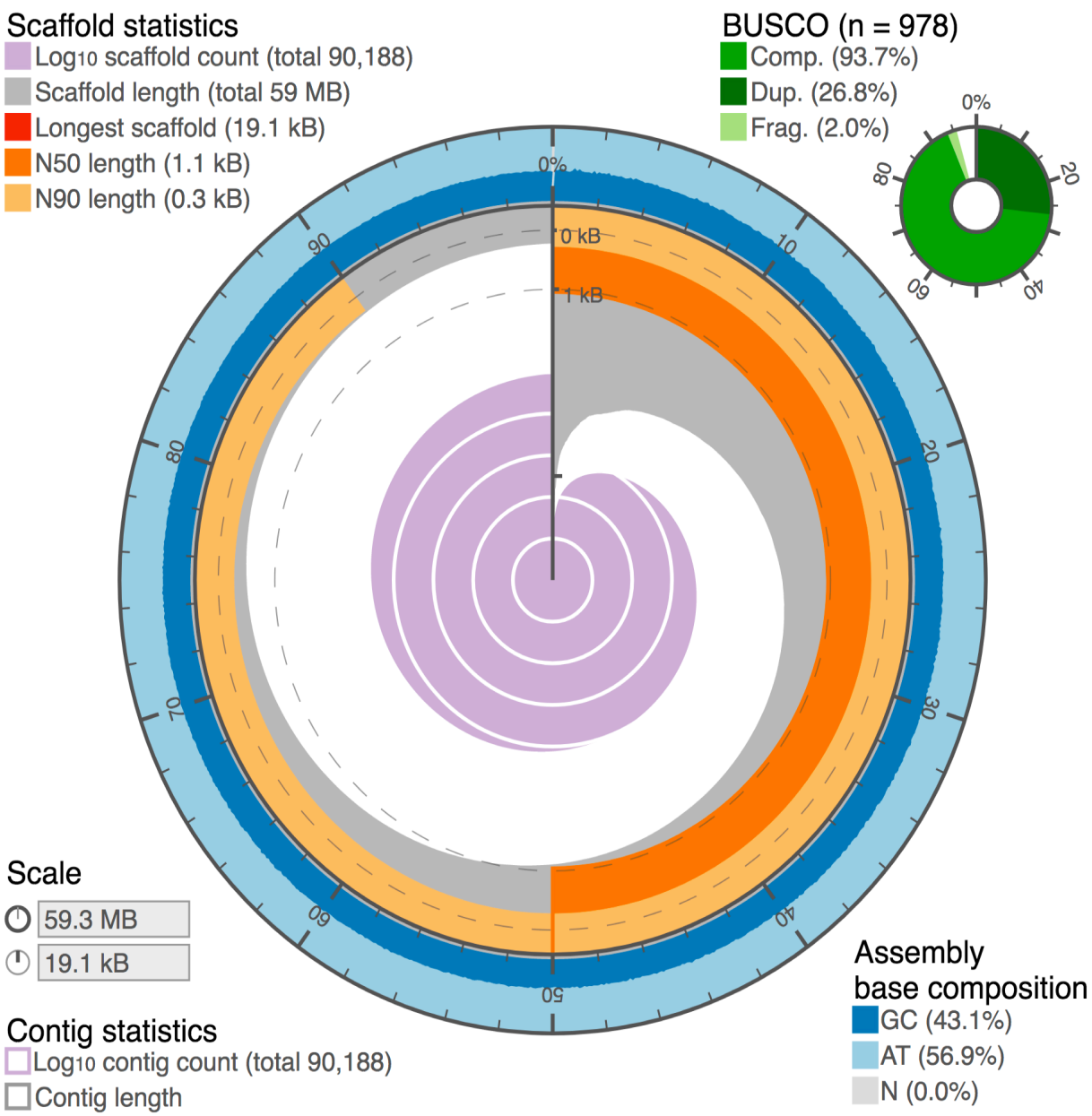

Figure 2: Summary of statistics related to assembly, including BUSCO results, contig size distribution and GC content, made using Assembly Stats tool (doi.org/10.5281/zenodo.322347). BUSCO results given top right. GC content represented with differential shading of outer blue circles, and is consistent across all contigs. Sizes of contigs, and the N50 size, are represented in inner circles as labelled at left, with logest contigs at “12 o’clock” position, and represented in order of decreasing size in a clockwise fashion.

bioRxiv preprint doi: https://doi.org/10.1101/416677; this version posted September 13, 2018. The copyright holder for this preprint (which was not certified by peer review) is the author/funder, who has granted bioRxiv a license to display the preprint in perpetuity. It is made available under aCC-BY-NC-ND 4.0 International license.

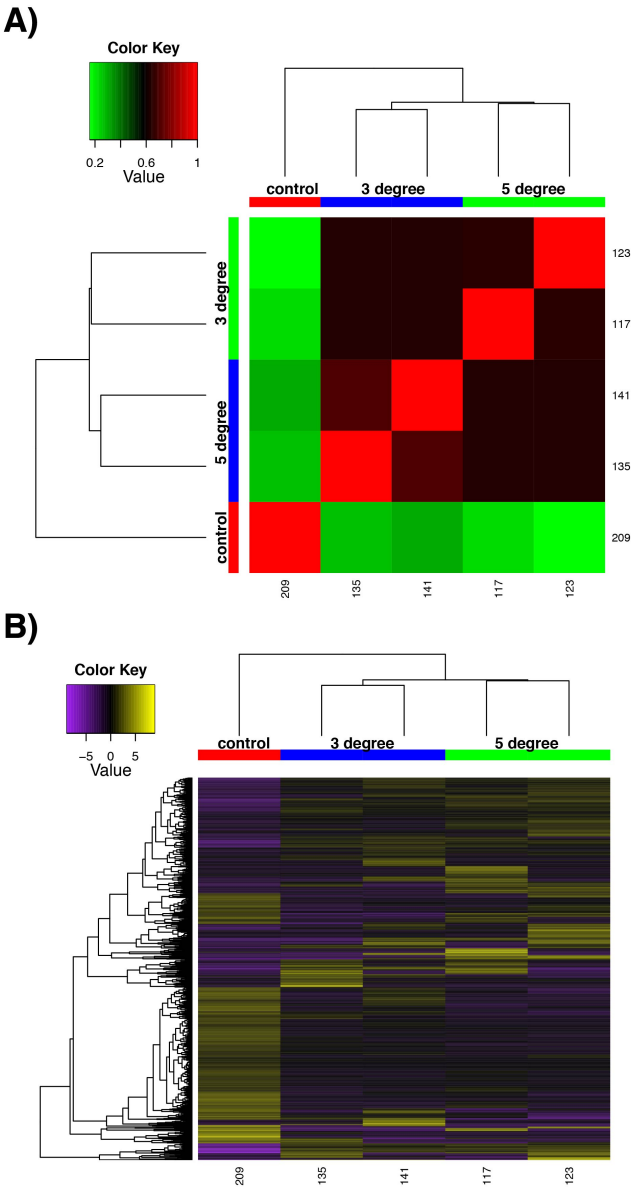

Figure 3: Differential expression analysis results performed by RSEM within the Trinity framework, with “as gene” results shown. A) is the sample correlation matrix for the five samples used in the final cross-comparison. B) shows the relative expression of each differentially expressed contig across all the samples. Note that contigs occurring uniquely in these samples are not included, as detailed in Methods. For both A and B, note the areas of the matrix shown in black hues, indicating few measurable differences between-samples.

bioRxiv preprint doi: https://doi.org/10.1101/416677; this version posted September 13, 2018. The copyright holder for this preprint (which was not certified by peer review) is the author/funder, who has granted bioRxiv a license to display the preprint in perpetuity. It is made available under aCC-BY-NC-ND 4.0 International license.

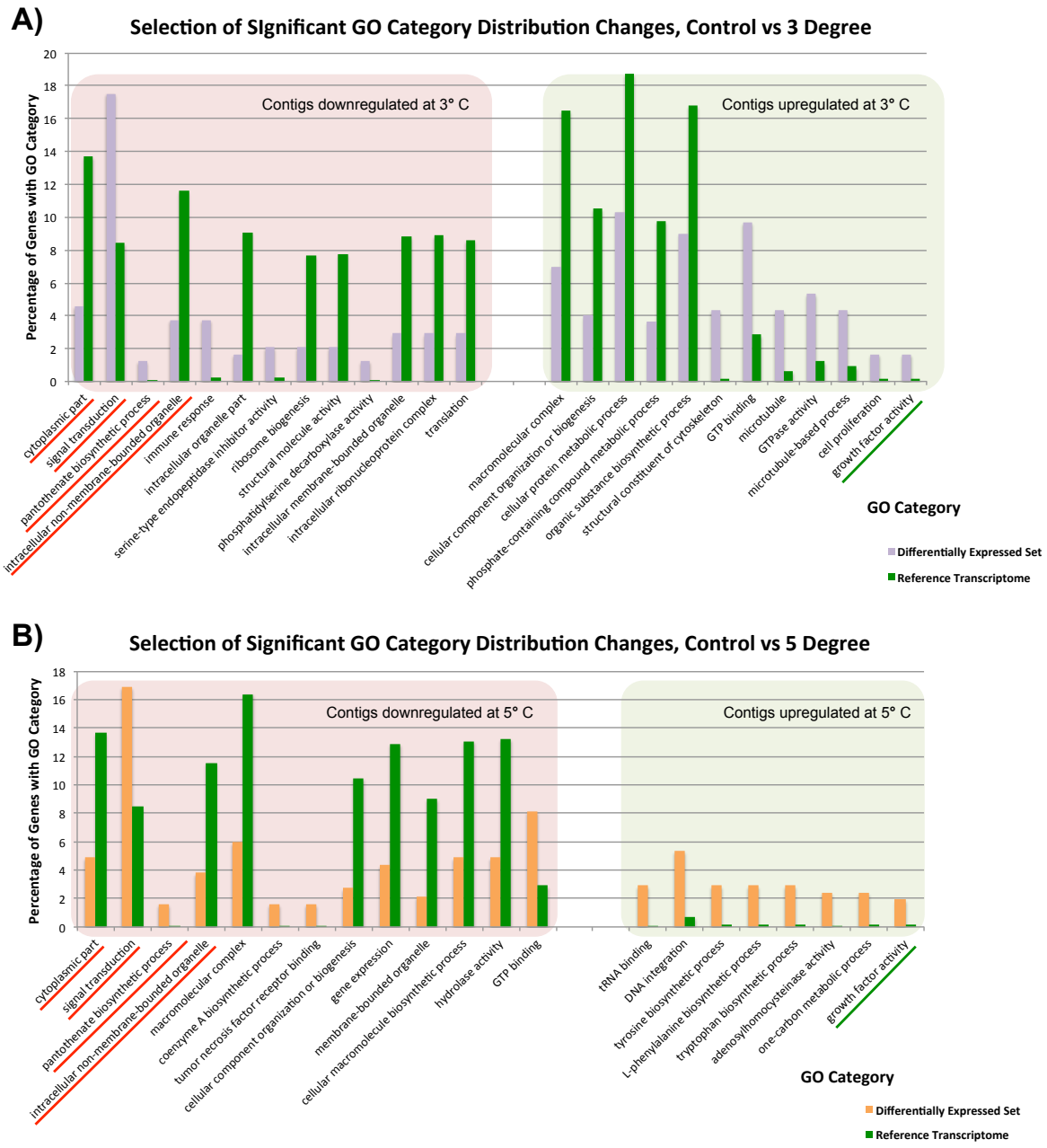

Figure 4: Significantly differentially represented GO categories from contigs up/down regulated at 3 and 5 °C compared to control sample. A) shows categories from our control vs 3 °C comparison, while B) shows those from the control vs 5 °C comparison. Those categories represented in both comparisons are underlined.

bioRxiv preprint doi: https://doi.org/10.1101/416677; this version posted September 13, 2018. The copyright holder for this preprint (which was not certified by peer review) is the author/funder, who has granted bioRxiv a license to display the preprint in perpetuity. It is made available under aCC-BY-NC-ND 4.0 International license.

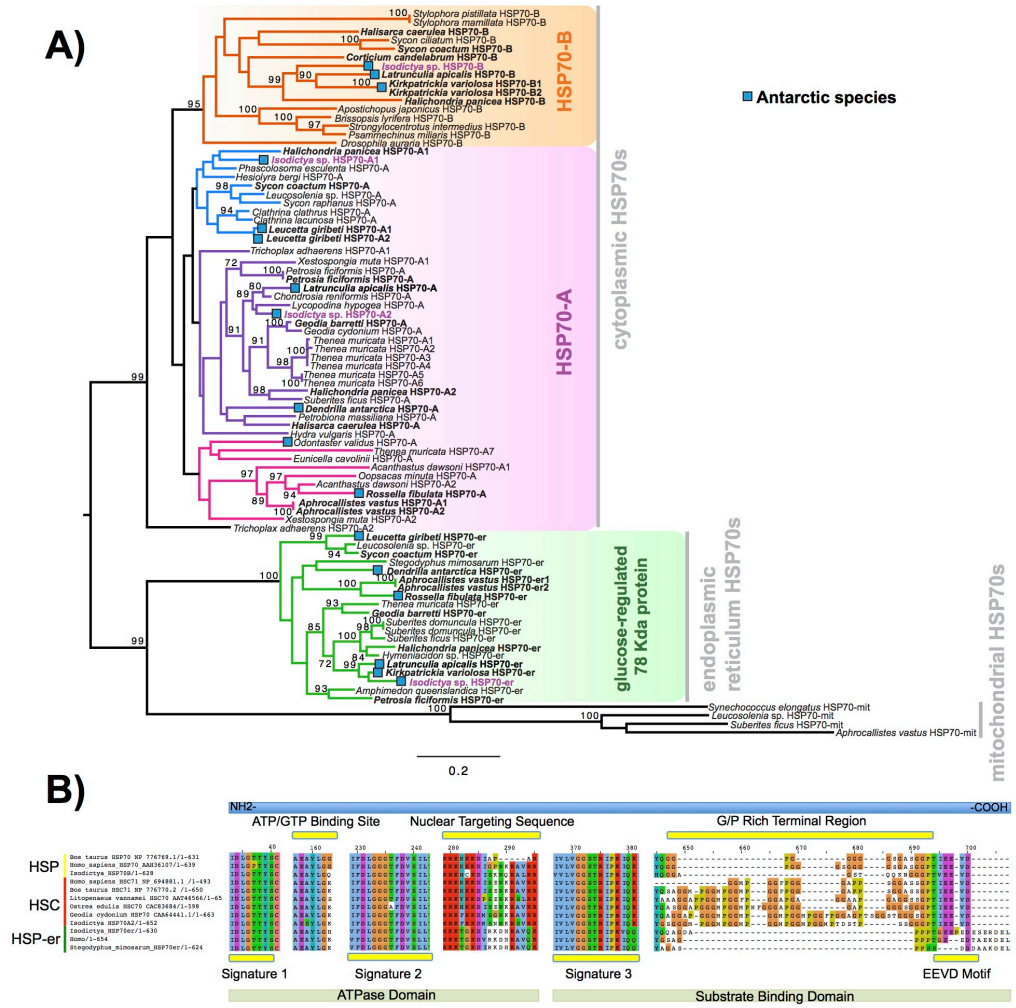

Figure 5: A) Maximum likelihood-derived phylogeny (RAxML, LG+I+G) of HSP70 sequences of known homology, together with novel *Isodictya* sequences (Names in purple). HSP70 sequences of Antarctic-resident species are bolded. Boxed as indicated on the figure are the HSP70-B, HSP70-A (HSC) and glucose-regulated 78 kDa HSP70 clades. Numbers at base of nodes indicate bootstrap support (as %ge of 1000 replicates). 5B: Multiple alignment of different HSP70 isoforms found in *Isodictya* sp. with (inducible) HSP70-B, sequence at top, HSP70-A (non-inducible heat-shock cognate) central, and below, HSP-mt sequences. These are shown alongside sequences from other species, showing the differences in domain content between isoforms. All HSPs have two main domains: the ATPase domain involved in ATP hydrolysis, and the substrate binding domain, which binds extended polypeptides, as shown at the bottom of the figure. Yellow boxes represent signature domains within HSP70 proteins. The G/P rich terminal region is prominent in HSPC (HSP-B). The EEVD sequence motif allows the cytoplasmic localisation of HSP and HSC isoforms. Accession numbers as provided in Figure, all sequences are provided, along with alignments, in Supplementary File 6.

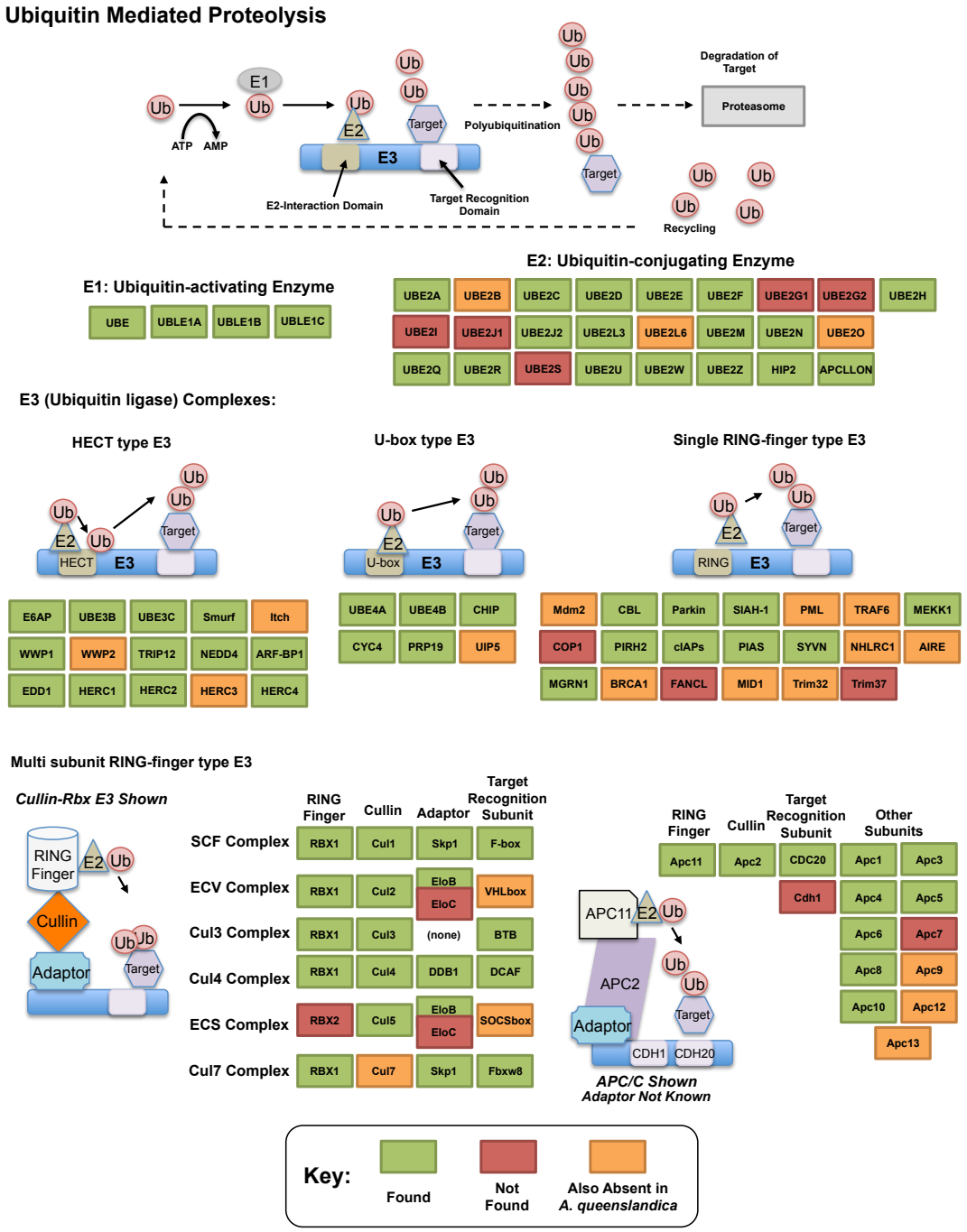

Figure 6: KEGG style map showing recovery of *Ubiquitin* mediated proteolysis genes in our resource as assessed by bi-directional best blast hit, alongside that of the sequenced genome of *Amphimedon queenslandica.* Genes noted as present in this resource indicated in green, with those absent in our transcriptome noted in orange if also missing from *A. queenslandica* (and therefore a possible poriferan absence), or red if absent from our resource only (and therefore a likely true absence).

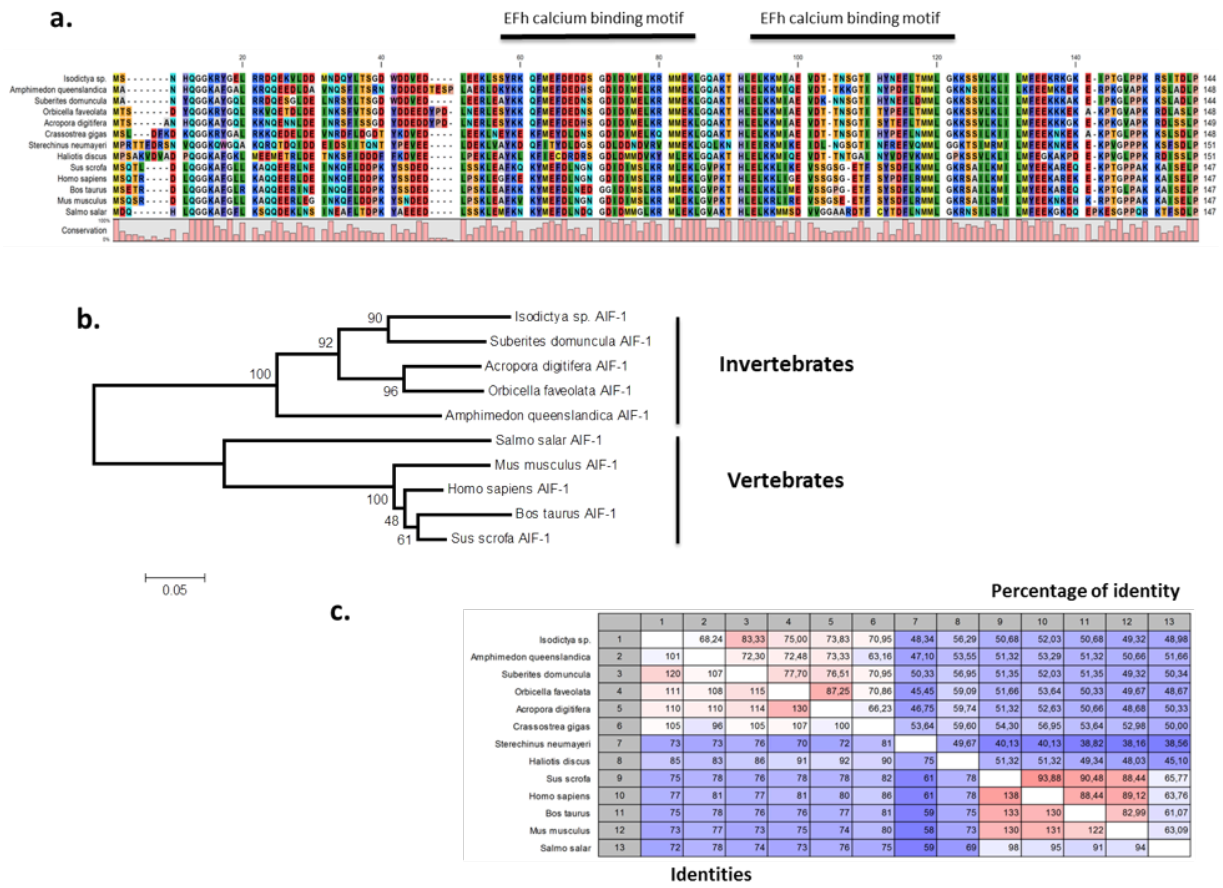

	1	2	3	4	5	6	7	8	9	10	11	12	13
Isodictya sp.	1		68,24	83,33	75,00	73,83	70,95	48,34	56,29	50,68	52,03	50,68	49,32	48,98
Amphimedon queenslandica	2	101		72,30	72,48	73,33	63,16	47,10	53,55	51,32	53,29	51,32	50,66	51,66
Suberites domuncula	3	120	107		77,70	76,51	70,95	50,33	56,95	51,35	52,03	51,35	49,32	50,34
Orbicella faveolata	4	111	108	115		87,25	70,86	45,45	59,09	51,66	53,64	50,33	49,67	48,67
Acropora digitifera	5	110	110	114	130		66,23	46,75	59,74	51,32	52,63	50,66	48,68	50,33
Crassostrea gigas	6	105	96	105	107	100		53,64	59,60	54,30	56,95	53,64	52,98	50,00
Sterechinus neumayeri	7	73	73	76	70	72	81		49,67	40,13	40,13	38,82	38,16	38,56
Haliotis discus	8	85	83	86	91	92	90	75		51,32	51,32	49,34	48,03	45,10
Sus scrofa	9	75	78	76	78	78	82	61	78		93,88	90,48	88,44	65,77
Homo sapiens	10	77	81	77	81	80	86	61	78	138		88,44	89,12	63,76
Bos taurus	11	75	78	76	76	77	81	59	75	133	130		82,99	61,07
Mus musculus	12	73	77	73	75	74	80	58	73	130	131	122		63,09
Salmo salar	13	72	78	74	73	76	75	59	69	98	95	91	94	

Figure 7: Alignment and phylogenetic analysis of the AIF sequences found in our transcriptome. A) The conserved two EF-hand motifs are indicated in the alignment of several AIF-1 from other invertebrate and vertebrate sequences; b) Phylogenetic tree of the AIF-1 family using the N-J method. Bootstrap values represent the frequency of appearance (expressed as a percentage) of each clade of 1000 bootstrap replicates; c) Percentage amino acid identities between AIF-1 genes from invertebrates and vertebrates. The GenBank accession numbers for the sequences are as follows: *Suberites domuncula* CAC38780; *Acropora digitifera* XP015755194; *Orbicella faveolata* XP020615825; *Amphimedon queenslandica* XP003387413; *Salmo salar* AC169994; *Mus musculus*; *Homo sapiens* P55008; *Bos taurus* NP001071547; *Sus crofa* P81076; *Crassostrea gigas* NP001292275; *Sterechinus neumayeri* ACO40483; *Haliotis discus* ABH10674.

Supplementary Files: https://figshare.com/s/0c90ae2e0b2a0524b036

Supplementary File 1: Reference transcriptome assembly (.fasta, zipped)

Supplementary File 2: Blast2GO annotation file incorporating Annex and Interproscan results (.annot, .b2g)

Supplementary File 3: KEGG KAAS annotation (.txt)

Supplementary File 4: Differential gene expression results (.txt, zip)

Supplementary File 5: Gene lists, overlapping in treatments (.txt)

Supplementary File 6: HSP70 phylogeny alignment (.phy, .fas, .nxs, zipped)

Supplementary File 7: Percentage identity comparison, HSP70 genes (.jpg)

Supplementary File 8: Antioxidant sequences